

High-Entropy Energy Materials in the Age of Big Data: A Critical Guide to Next-Generation Synthesis and Applications

Qingsong Wang, Leonardo Velasco,* Ben Breitung,* and Volker Presser*

High-entropy materials (HEMs) with promising energy storage and conversion properties have recently attracted worldwide increasing research interest. Nevertheless, most research on the synthesis of HEMs focuses on a “trial and error” method without any guidance, which is very laborious and time-consuming. This review aims to provide an instructive approach to searching and developing new high-entropy energy materials in a much more efficient way. Toward materials design for future technologies, a fundamental understanding of the process/structure/property/performance linkage on an atomistic level will promote pre-screening and selection of material candidates. With the help of computational material science, in which the fast development of computational capabilities that have a rapidly growing impact on new materials design, this fundamental understanding can be approached. Furthermore, high-throughput experimental methods, enabled by the advances in instrumentation and electronics, will accelerate the production of large quantities of results and stimulate the identification of the target products, adding knowledge in computational design. This review shows that combining computational preselection and verification by high-throughput can be an efficient approach to unveil the complexities of HEMs and design novel HEMs with enhanced properties for energy-related applications.

saying “technology is always limited by the materials available” still holds true today.^[1] Therefore, developing and optimizing new materials will remain of tremendous importance in the coming years. This particularly applies in the light of ever-increasing performance requirements and a transition toward more effective and more sustainable technologies. Based on the functionality of these materials, vital tasks could be executed more efficiently, and tools could be manufactured, which by themselves supported the further search for even more sophisticated materials. The strive for materials to execute more complicated tasks demands an increased complexity of the materials; therefore, people started mixing different components, preparing the first complex alloys and composite materials already at an early age of history. Nowadays, very complex materials with various incorporated elements are known and used for a wide variety of different applications. Well-known examples

1. Introduction

The discovery and development of novel materials have always accompanied technological progress. Nevertheless, the 1960s

for such materials with many different incorporated elements are found in the field of electrochemical energy storage (batteries) with electrodes composed of layered delafossite structures, such as NCM ($\text{Li}(\text{NiCoMn})\text{O}_2$), $\text{Li}(\text{NiCoAl})\text{O}_2$, or the spinel $\text{LiNi}_{0.5}\text{Mn}_{1.5}\text{O}_4$.^[2]

A similar trend toward a more complex composition to enable better and tailored performance is seen for the rapidly growing material family of MXene,^[3] which are 2D metal carbides/nitrides/carbonitrides with the unique ability to form solid solutions while maintaining their nanolamellar structure.^[4] MXenes are obtained from removing A-site atoms from the MAX phase crystal lattice; we find for MAX phases $\text{M}_{n+1}\text{AX}_n$ ($n = 1-4$), where M represents an early transition metal element (e.g., V, Nb, Ti, Cr), A is an element typically from group 13 or 14 (e.g., Si, Al, Ga, Ge), and X is C and/or N.^[4,5] MXenes have already demonstrated their tailored properties. For example, Han et al. studied the Ti–V–Nb MXene system^[5] and effectively modified electronic and optical properties. The properties of MXenes are also greatly influenced by the surface groups, often referred to as T_x or T_z ; they strongly impact the electronic, electrochemical, and electrocatalytic properties.^[6] Tailored surface functionality can also be seen as one more “element” to modify in addition to the chemical modification of the M- and X-site atoms.


A temporary peak of materials complexity was developed independently by Cantor and Yeh, who both described the formation of an equimolar multi-element single-phase alloy,

Q. Wang, V. Presser
INM—Leibniz Institute for New Materials
Campus D2 2, Saarbrücken, Germany
E-mail: volker.presser@leibniz-inm.de

Q. Wang, L. Velasco, B. Breitung
Institute of Nanotechnology
Karlsruhe Institute of Technology
Hermann-von-Helmholtz-Platz 1, 76344 Eggenstein-Leopoldshafen, Germany
E-mail: leonardo.estrada@kit.edu; ben.breitung@kit.edu

V. Presser
Department of Material Science and Engineering
Saarland University
Campus D2 2, Saarbrücken, Germany

V. Presser
Saarene—Saarland Center for Energy Materials and Sustainability
Campus D4 2, Saarbrücken, Germany

 The ORCID identification number(s) for the author(s) of this article can be found under <https://doi.org/10.1002/aenm.202102355>.

© 2021 The Authors. Advanced Energy Materials published by Wiley-VCH GmbH. This is an open access article under the terms of the Creative Commons Attribution License, which permits use, distribution and reproduction in any medium, provided the original work is properly cited.

DOI: 10.1002/aenm.202102355

FeCrMnNiCo.^[7,8] A new concept of alloying strategy to create new materials involving the combination of multi-principal atomic elements in high concentrations has thus been raised. Although alternative names, such as multi-component alloys, compositionally complex alloys, and multi-principal-element alloys, were suggested, this material class was later framed as high-entropy alloys (HEAs) based on simplification.^[9,10] However, despite high entropy being favorable to enhance the formation and stability of random single-phase solid solution in a specific structure, entropy is not necessarily the prime factor dominating the structure and related properties.^[11] HEAs have triggered the following-up rapid development of high-entropy ceramics (HECs), like high-entropy nitrides (2006)^[12] and carbides (2010),^[13] high-entropy oxides (HEO; 2015),^[14] and high-entropy MXenes (2021).^[15] The inspiring work of HEO shows a single-phase rock-salt structure with equimolar cations on the cationic sublattice, which can be seen as the starting point for various subsequent studies about HECs. Consequently, the term “high-entropy materials” (HEMs) is nowadays used as an umbrella term to describe the whole variety of different high-entropy compounds in materials science. The HEMs are based on increasing the configurational entropy (S_{config}) as much as possible to, in some cases, obtain entropy stabilization and exploit the resulting cocktail effects that describe the condition that often a mixed material is more than just the sum of its individual parts. The cocktail effects describe the interplay of the different elements in one single-phase structure, highlighting the importance of every participating element.^[16] When the elemental composition or the stoichiometry of a HEM is changed, the material properties might vary enormously due to the changing interactions of the various incorporated elements. Therefore, it is also possible to tailor the properties by the right choice of elements and stoichiometries. In this regard, the high-entropy concept describes the strategy to include various elements in a single-phase structure to exploit the changed properties arising from the resulting cocktail effects, lattice distortion, and, if apparent, entropy stabilization. Since incorporating many different elements automatically results in a high configurational entropy, this concept is coined as “high-entropy concept” and limited to materials with a configurational entropy above 1.5R, not necessarily including entropy stabilization.

HEMs have gained significant interest and emerged rapidly for energy-related applications, such as energy storage, electrocatalysis, and sensors. However, with increased complexity, the targeted development and optimization of a specific property becomes more complex. Due to the cocktail effects, small changes in composition or stoichiometry can significantly alter properties, severely complicating predicting the material's behavior by simple chemical understanding. Therefore, the high-entropy concept allows for entirely novel material compositions and uniquely tailors the materials' properties. Still, it impedes a straightforward optimization of desired properties and the development of specific functional materials simply by offering too many possibilities to prepare the highly complex system and the cocktail effects' unusual behavior even at small compositional changes.

The high-entropy concept paves the way for entirely new functional materials with distinctive and tailorable properties. However, it is challenging to perform a directed search for a

specific functionality due to the compositional complexity. Several comprehensive reviews on HEMs for energy-related applications have already been published.^[9,17–20] Therefore, we focus on the description and the development of strategies to find the most efficient way to identify the proper compositions and stoichiometries of HEMs to optimize specific desired properties. This review will present an overview of the approaches developed to optimize the efficiency of directed research to prepare HEMs with suitable composition and stoichiometry for a given property. To do that, this review guides through the jungle of infinite HEM compositions and synthesis methods and presents exemplified literature along this way. The focus of the properties of the materials will be set to energy-related applications and the different strategies to obtain high performances and optimize certain features of the material. A guideline on successfully preparing such HEMs, with a future perspective on increasing the efficiency to find the suitable composition, will be drawn over the different chapters and a clear picture of the different strategies in the existing literature presented. The chapters will describe the techniques of “trial and error,” “directed research,” “computational design,” and “high-throughput” and explain the connections and the state-of-the-art of the different topics. A timeline of the evolution, key application aspects, and possible optimization of materials design in the field of HEMs are presented in **Figure 1**. The emergence of HEAs in 2004 was followed by an extensive investigation of their mechanical properties, since their structure is believed to be stabilized by the maximized configurational entropy through the highly disordered incorporated elements. With the discovery of the entropy-stabilized oxides in 2015, the development of many other HEMs for energy-related applications followed over the years. With modern computational calculations, which can shed light on the relationship between the local electronic structure and the properties of the material, and emerging advanced synthesis techniques, promising opportunities are provided to explore novel HEMs in a much efficient way.

2. “Trial and Error” and “Directed Research”

As for many other considerable developments, the first HEA compositions were found using a “trial and error” approach. In 2004, Cantor et al. investigated the microstructures of a cooled alloy, prepared by melt spinning of a 20 metal and semi-metal containing melt.^[7] The result was the predominant face-centered cubic (fcc) solid solution FeCrMnNiCo, composed of equimolar proportions of the respective elements. The surprising finding was that most individual metals would not form fcc structures when crystallized independently, but an entropy stabilization facilitated the formation of a single-phase fcc structure when mixed. Independently, Yeh et al. reported in the same year a CuCoNiCrAl_xFe alloy system, prepared by arc melting, tested different Al concentrations and investigated the impact of this concentration on the mechanical and structural properties.^[8] These two studies can be seen as the birth of the HEAs, a term framed by Yeh and that has ever since become widely accepted and used by the majority of the community.

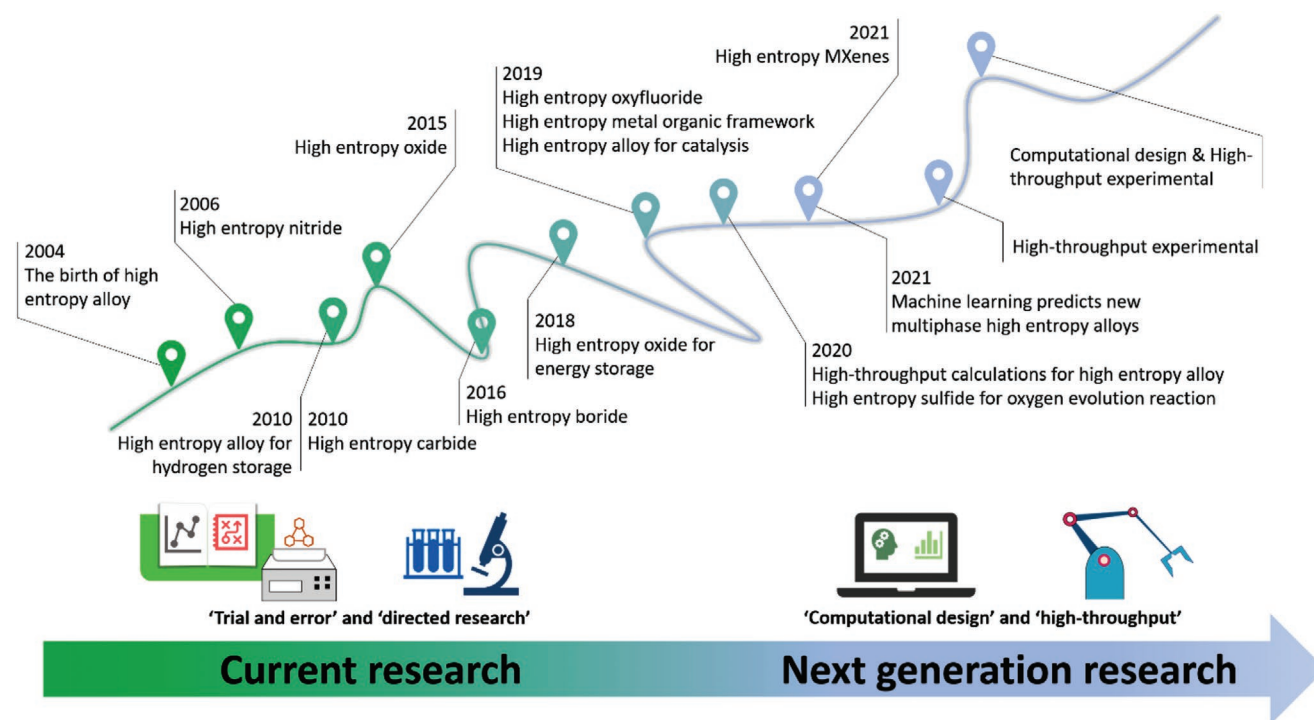


Figure 1. Timeline of the development of HEMs and some key applications. Experiments through “trial and error” or “directed research” approaches dominate the current work on HEMs, and the computational design and high-throughput experimental are just beginning to play a role. Applications of HEMs cover many fields, including engineering, energy storage, and conversion.

These two initial studies exemplify the conceptual differences between “trial and error” and “directed research.” The conducted experiments to form the first HEAs were not directed to a specific composition or based on predictive tools, and the results were a priori unknown accordingly. Owing to the vast amount of possible compositions and stoichiometries, the “trial and error” approach was very reasonable to find the first possible combinations of HEAs. The experiments to change the concentration of only one element can be seen as the first approach to tailor the HEAs’ properties and change the features by “directed research.”

In 2015, Rost et al. applied the high-entropy concept for the first time to oxidic ceramics, preparing the first HEOs.^[14] These HEOs initiated a boost in the research of HECs and were prepared by “directed research.” The idea was to follow the Goldschmidt rules, which describe a model to increase the chance to obtain stable phases and structures when preparing materials with mixed elements.^[21] Many more combinations for different ceramics were reported from this study, including sulfides, fluorides, oxyfluorides, nitrides, carbides, borides, and metal-organic frameworks.^[20,22]

The utilization of HEMs for energy applications started with the attempt to use HEAs as hydrogen storage materials. Kao et al. chose CoFeMnTiVZr, a C14 Laves structure with the known ability to store hydrogen reversibly, and used a “directed research” approach to optimize the kinetics and storage capacity by changing the concentrations of Ti, V, or Zr.^[23] Additionally, HEAs’ superior physicochemical stability and extraordinary mechanical properties, conspicuously the notable catalytic activity and excellent durability, make them very promising for

electrocatalytic application.^[24] Minimizing the usage of noble metals or even making their use obsolete would be a highly cost-effective alternative route for catalysts. Löffler et al. demonstrated the utilization of “Cantor alloy” CoCrFeMnNi HEA nanoparticles as an oxygen reduction reaction catalyst, which does not contain noble metal while shows intrinsic activity comparable to Pt.^[25] In this study, through “directed research”, the necessity of a combination of all the five principal elements was verified by removing each element from the quinary HEA system.

The first indications that HEMs show promise for electrochemical energy storage applications appeared after the introduction of HECs. Since then, many reports have focused on using HECs as electrode materials or electrolytes for ionic transport. Most of the studies took existing compositions in a “trial and error” approach or selectively chose redox-active elements and incorporated them using a “directed research” technique. The choice of elements to prepare reasonable electrochemically active HECs was based on the experience gathered from known nonhigh-entropy compounds. For electrode materials, especially composed of late transition metals such as Mn, Co, and Ni, which are well-known in common secondary battery materials like LiCoO₂ (LCO) or Li(NiCoMn)O₂, are reasonable choices for the design of high-entropy active materials for electrochemical energy storage applications. Both the “trial and error” and the “directed research” approach appeared often combined: first, a promising composition was found, and then one or two elements were replaced by other more promising elements to improve the material’s performance.

The infinite amount of different composition possibilities in HECs causes a difficult decision to synthesize and investigate the electrochemical properties. The first experiments were performed using (CoCuNiMgZn)O by Rost et al., with each cation being present in equimolar ratios on the cationic sublattice of a rock salt structure. Bérardan et al. took this composition as a starting point, tested the dielectric constant and the Li-ion conductivity.^[26] The intention to study the dielectric properties of the compound was plausible since all binary oxides are electrical insulators. Still, the bandgap was expected to be not just an average. The starting point, using (CoCuNiMgZn)O as an initial sample, can be considered as a “trial and error” experiment to test the properties of a new compound, the subsequent strategic tailoring with Li and Ga, as a “directed research” approach to find out about charge compensation mechanisms and to optimize the Li-ion conductivity of the materials.^[27]

Later, many more studies reported using HECs for electrochemical energy storage, but all had to make the difficult decision, which composition to take and which elements to replace to tailor the materials. Since slight variation in composition can result in significant changes in properties due to complex interactions of the incorporated ions, the results of a tailoring approach can often not be predicted. Additionally, the interactions of the ions and structural changes, such as Jahn–Teller distortions or the breaking of low range ordered structures, can affect the electrochemical properties of HECs.^[28,29] Therefore, most reported results are based on “trial and error” approaches, while only a few explore “directed research” processes. The already described rock-salt structured (CoCuNiMgZn)O was also the subject of many other reports about electrochemical properties so that this compound can be seen as the point of reference for research on HECs for electrochemical energy storage and conversion.

The first report on (CoCuNiMgZn)O used for active electrode materials described the conversion reaction behavior of the compound, which shows extraordinary capacity stabilities with continuous cycling compared to binary and medium entropy ($S_{\text{config}} < 1.5R$) materials.^[19,30] For “trial and error”, the compound was tested to establish the general electrochemical behavior, and later the role of entropy and the individual elements were investigated by systematically altering the materials composition. Eliminating elements has a significant effect on stability and redox potential, but the impact of a specific element could not be predicted or derived. Qiu et al. could even present increased capacities by changing the morphology of the particles by ball-milling and could present indications for increased structural stability of a (CoCuNiMgZn)O electrode compared to conventional conversion materials.^[31]

Further research focused on improving the capacity by applying different strategies. By transferring the concept to increase the oxygen vacancies in an anode material to change the electrochemical properties, a “directed research” experiment was done, which modified the composition of (CoCuNiMgZn)O by extracting Cu and introducing Li to form (CoNiMgZn)_xLi_{1-x}O.^[32] Other studies connected the grain size and surface area to the capacity since there is an increased capacity compared to the original material.^[33] The complex composition of the (CoCuNiMgZn)O and the related compounds impede a precise determination of the reaction mechanism. Only with the help of

operando X-ray absorption spectroscopy and differential electrochemical mass spectrometry, more information about the electrochemical reactions of the material in a cell could be gathered, leading to the conclusion that a complicated combination of alloying and conversion reactions appear based on the incorporated elements.^[34]

Despite the experimental efforts to optimize the electrochemical properties, it remains unclear if the ideal composition for rock-salt high-entropy conversion electrodes requires exactly all five cations of the (CoCuNiMgZn)O system. Due to the vast number of different combinations possible for HE rock-salt metal oxides structures, there is an infinite number of possible combinations, which cannot be experimentally explored by using “trial and error” or “directed research”. Solely for the single-phase rock-salt structured compounds, M was reported to be Co, Ni, Cu, Zn, Mg, Fe, Cr, Mn, Li, Ga, Mo, and many more.^[35] The possible number of combinations of only this one structure, not to speak of changed stoichiometries in a specific composition, makes it impossible to test all promising variations. Therefore, the search for possible combinations is very time-consuming and inefficient. The probability of much more viable combinations of cations and anions existing for electrochemical applications is extremely high. Despite transitioning from “trial and error” to “directed research” narrows the combinations down, elemental interactions, which might appear in complex systems but are not easily recognizable for scientists, are not adequately considered.

Besides the rock-salt structured HECs, other crystal structures were investigated as well for other battery types. Most of the research is based on “trial and error” since no comparable systems were available, leaving much room for improvement using other compositions or stoichiometries. One of those structures is the spinel structure, which even holds more promise for conversion materials, since the redox states of the incorporated metal ions are higher than for rock-salt structures. These spinel structures are mixed-valence compounds, meaning that M^{2+} and M^{3+} ions occupy the cationic sublattices. Several different compositions, (MgTiZnCuFe)₃O₄, (NiCoMnFeTi)₃O₄, (CoCrFeMnNi)₃O₄, and (CoCrFeMnNiAl_{0.038})₃O_{4-x}, were explored and the electrochemical performance was measured.^[36] The reports about the capacity and reversibility are very similar between (MgTiZnCuFe)₃O₄ and (NiCoMnFeTi)₃O₄ and between the compounds (CoCrFeMnNi)₃O₄ and (CoCrFeMnNiAl_{0.038})₃O_{4-x}. The reasons are most likely particle size issues since the X-ray diffractograms for the latter materials showing higher capacity indicate smaller domain sizes due to the different synthesis procedures. Other spinel compounds were reported, including toxic elements like (BeMgCaSrZnNi)₃O₄, and perovskites for lithium-ion and lithium-sulfur batteries.^[37]

These results show that it is often uncertain if the improved properties arise from the different stoichiometry and composition of the HEMs or if the particle size and morphology play a much more decisive role. Therefore, it is imperative to compare the properties of HEMs with similar non high-entropy materials, for example, the binary compounds or low- to medium-entropy materials. To trace the properties back to the elemental interactions, it is also essential to keep the crystal structure and replicate the particle morphology and the preparation method since all these factors would complicate a comparison if not

similar. It is difficult to find such comparable materials; still, if found, then the low- or medium-entropy type of the material can be prepared using the same approach as the HEM while keeping the number of different elements low.

This strategy was employed by certain different groups and gave a deep insight into the properties arising with applying the high-entropy concept. The most used cathode active material in rechargeable batteries on the market are layered structured intercalation materials like LCO or NCM. NCM is an example of introducing multiple elements into a single-phase structure to exploit the interactions of the different elements. Here, Ni and Mn's introduction to LCO leads to improved reversibility and decreased costs (replacing expensive Co). Additionally, stoichiometry can be tailored regarding the needs of the battery, NCM compositions with Ni:Co:Mn ratio of 1:1:1, 6:2:2, and 8:1:1 are investigated or already widely used.

Until now, two different types of high-entropy layered oxides are reported, a series of $\text{Li}(\text{NiCoMnAlFe})\text{O}_2$ type materials for Li batteries and O3-type sodium-based layered oxide $\text{NaNi}_{0.12}\text{Cu}_{0.12}\text{Mg}_{0.12}\text{Fe}_{0.15}\text{Co}_{0.15}\text{Mn}_{0.1}\text{Ti}_{0.1}\text{Sn}_{0.1}\text{Sb}_{0.04}\text{O}_2$ for reversible sodium intercalation.^[38,39] In both materials, the high-entropy should be created on the transition metal layers of the structures, for Li intercalation (NiCoMnAlFe) replaces (NiCoMn) as known in NCM CAMs and for Na-ion intercalation, $\text{Ni}_{0.12}\text{Cu}_{0.12}\text{Mg}_{0.12}\text{Fe}_{0.15}\text{Co}_{0.15}\text{Mn}_{0.1}\text{Ti}_{0.1}\text{Sn}_{0.1}\text{Sb}_{0.04}$ replaces (NiFeMn) as known for a common O3-type Na-ion insertion material like $\text{Na}(\text{NiFeMn})\text{O}_2$. Using “directed research”, the careful selection of the incorporated elements suppressed the typical P3-to-O3 phase transition that appears in other Na intercalation materials and decreases the reversibility of the reaction.^[40] When using equimolar transition metal cations for the high-entropy Li intercalation material $\text{Li}(\text{NiCoMnAlFe})\text{O}_2$, the redox reaction almost vanished but could be restored by introducing Na in the parent lattice, forming $\text{LiNa}(\text{NiCoMnAlFe})\text{O}_2$. It was impossible to exclude Li-ion migration into the transition metal layers, so cation intermixing appeared strongly and impeded the capacity.

Lun et al. provided another example of how the high-entropy approach influences the structure and structural changes during reversible Li-insertion.^[29] They applied the strategy to compare the HEMs with medium- or low-entropy compounds and found that a particular short-range order, which is apparent medium- or low-entropy distorted rock-salt structures, could be broken by introducing a high number of elements. This short-range order blocked Li-pathways; therefore, the capacity was strongly improved with an increased number of cations. Similar materials as the here used high-entropy oxyfluorides were prepared in a different composition earlier and used for insertion CAMs. In this example, for the first time, a HEM with several cations on the cationic sublattice and several anions on the anionic sublattice was prepared by simple ball-milling of the already discussed $(\text{CoCuNiMgZn})\text{O}$ with LiF .^[20] The material, $\text{Li}(\text{CoCuNiMgZn})\text{OF}$, showed improved performance compared to $\text{Li}(\text{Ni})\text{OF}$, which was explained later by Lun et al.^[29] The result of the cocktail effects and the mixing of different elements could be shown exemplary here, where the simple transition of a high-entropy rock-salt oxide to a high-entropy rock-salt oxyfluoride results in a change from an anode to a cathode material.

These examples show that applying the high-entropy approach on different crystal structures can lead to different outcomes, which are strongly related to the materials' elemental interactions and structural changes. This makes it even more challenging to design a strategy to improve a particular property of a HEM efficiently. The position of most HEMs in the middle of a multi-dimensional phase diagram opens a huge chemical phase space, which, combined with the impact of structural changes on the properties, enables countless possibilities for functional materials. Using the “trial and error” or the “directed research” approach makes it impossible to state if the optimal combination of elements or the optimal structure resulting from the high-entropy approach is found. Additionally, determining the correct elements to exchange, add or subtract to optimize a specific electrochemical property presents an equal challenge. Due to these reasons, other approaches had to be explored to find the most promising elements and stoichiometries in HEMs. These will be described in the following sections.

3. Computational Design

Significant progress has been achieved on an experimental basis in “trial and error” or the “directed research” approach. Nevertheless, these two traditionally experimental methods require intensive time and cost for experimental evaluations, particularly without any guidance or prescreening, and cannot meet the fast development of the next-generation energy materials with advanced performance. Therefore, efficient and effective scientific strategies that boost the design and discovery of high-entropy energy materials are needed. Future feasible attempts should address the complexity in physics and chemistry when searching for materials correlations, understanding materials chemistry, and targeting specific applications. Computational data-driven material discovery enables the accelerated development of new materials, while experimental data is often sparse with limited chemical space coverage. The density functional theory (DFT) calculation, a computational quantum mechanical modeling method, has been used for screening new materials during the last few decades.^[41] Machine learning, a subfield of artificial intelligence, has recently become an efficient tool for analyzing existing materials that would revolutionize scientific discoveries to develop energy materials.^[42] It is anticipated that the use of theoretical and computational chemistry to predict quantitative structure-property relationships before experiments will promote further developments of HEMs in energy storage and conversion.^[43] This section will discuss energy-related HEMs for which computationally aided material design methods have been successfully applied.

One of the most prevalent strategies for improving materials' properties is lattice doping. Ever since the advent of the commercializing of the LCO cathode, extensive efforts have been devoted to searching for cheaper, structurally more stable, and safer alternatives. For improving phase stability, cationic doping has been carried out experimentally in “trial and error” by choosing different single dopant or even dopant pairs, such as Al, Fe, Mg, Ti, or Zr and Al–Mg, Mg–Ti, or Mg–Ga.^[44] Al substitution has been widely deployed for alleviating structural

deformation at deep charge states. The first computational revolution in material science was driven primarily by DFT calculations, which tailor functional parameters to reproduce experimental results.^[45]

At an earlier state for searching a cathode alternative for LCO, first-principal calculations have demonstrated its instructive predictive potential.^[46] In 1998, Ceder et al. predicted and verified experimentally that aluminum substitution in novel cathode material $\text{LiAl}_x\text{Co}_{1-x}\text{O}_2$ could increase energy density while reducing the cost.^[46] The ab initio computation discovered the intercalation voltage of Li_xAlO_2 to be 5.4 V, and LiAlO_2 as a solid solution component will lead to higher Li intercalation voltage. Single-phase solid solution (space group $R\bar{3}m$) with $x \leq 0.5$ showing higher equilibrium open-circuit voltage was then verified experimentally. This pioneering work has inspired hereafter broad interest in computational calculation and experimental, although an optimized limited amount of Al within 5 at% is generally considered.^[47]

A recent study from Zou et al. on Ni-rich cathode $\text{LiNi}_{0.92}\text{Co}_{0.06}\text{Al}_{0.02}\text{O}_2$ investigated the electrode electronic structure change induced by Al substitution using DFT calculations, revealing not only the improved bulk stability but also the interfacial, which has also been proofed experimentally.^[48] In addition to the single-doping strategy, a multicomponent-doping approach has been proposed in Ni-rich NCM cathodes by understanding the atomic and electronic structure with the first-principles DFT calculations dopants.^[49] The influence of seven cations (Mg, Al, Si, Ti, V, Ga, and Zr) was systematically assessed.^[49] Positive effects of dopants can be divided into two distinct categories: phase stability during materials synthesis and reversibility during electrochemical cycles. This multicomponent-doping strategy is on its way to complex compositions or approaching rational high-entropy approach direction, as not a single dopant can solve all the problems simultaneously.

Traditionally, for the cathode materials capable of fast lithium-ion diffusion, the atomic configuration in the crystal structure must be in well-layered ordering. The disordering in the crystal structure is much overlooked. Recently, with the introduction of the 3D lithium-ion percolation theory (lithium migration occurs between neighboring octahedral sites via an intermediate tetrahedral activated state, referred to as o–t–o diffusion), disordered rock-salt (DRX) structure cathodes are receiving significant attention due to their high capacity compared with ordered layered cathode materials.^[20,29,50] In the ideal DRX structure, Li and other metal elements are distributed randomly in the rock-salt cation sublattice in a single phase (space group $Fm\bar{3}m$). Therefore, cations in DRX materials do not have a long-range periodic arrangement and intrinsically hold more diverse local environments. As mentioned above, the high-entropy concept was applied to DRX cathodes by Ceder's group.^[29] Improved capacity and decreased polarization have been demonstrated owing to increased lithium-ion transportation, which enabled the suppressed short-range order resulting from the increase of cationic species in the high-entropy cathode. High-entropy $\text{Li}_{1.3}\text{Mn}_{0.1}^{2+}\text{Co}_{0.1}^{2+}\text{Mn}_{0.1}^{3+}\text{Cr}_{0.1}^{3+}\text{Ti}_{0.1}\text{Nb}_{0.2}\text{O}_{1.7}\text{F}_{0.3}$ shows the highest specific capacity of 307 mAh g^{-1} and most stable cycling performance at improved charge/discharge rates with comparison to medium-entropy $\text{Li}_{1.3}\text{Mn}_{0.2}^{2+}\text{Mn}_{0.2}^{3+}\text{Ti}_{0.1}\text{Nb}_{0.2}\text{O}_{1.7}\text{F}_{0.3}$

and low-entropy $\text{Li}_{1.3}\text{Mn}_{0.4}^{3+}\text{Ti}_{0.3}\text{O}_{1.7}\text{F}_{0.3}$. The introduction of the high-entropy concept reduces or ideally eliminates the short-range cation order and further broadens the chemical space of DRX compounds. Specifically, a total of 23 metal cations were considered for compatibility analysis (Figure 2a) by first-principles DFT calculations, creating 7965 distinct compounds. Moreover, in the dataset created by the DFT calculations, low short-range order compounds with suitable chemistries could also be predicted, and a HE DRX compound with a large number of 12 cationic species in similar concentrations was successfully prepared as a proof of concept. The phase purity and homogenous distribution of different elements were also demonstrated, as shown in Figure 2b.

In a high-entropy system, the involvement of multi-component compounds allows them to form a single-phase solid solution with a simple crystal structure because of the high configurational entropy. The extraordinary properties of HEMs are appealing, while the predictions of multiple competing phases or phase separation are still challenging. DFT-based first-principles calculations have been used for theoretically demonstrating the formation possibility and stability phase stability of new HECs or HEAs.^[51,52] Ye et al. demonstrated the experimental fabrication of high-entropy carbide $(\text{Zr}_{0.25}\text{Nb}_{0.25}\text{Ti}_{0.25}\text{V}_{0.25})\text{C}$, which was initially analyzed by combining first-principles calculations and thermodynamical study.^[52,53] Feng et al. predicted the phase stability in the quaternary Cr–Mo–Nb–V alloy system, in which the configurational entropy plays a critical role.^[53] Then, the entropic stabilization of HEAs has been shown experimentally by the phase transformation between annealing treatment at low and high temperatures. However, a low computational cost has been a significant challenge in ab initio computational materials science. The random distribution of the atoms may induce considerable challenges in building an atomic model, and as a result, this creates difficulty in guiding the constitution combinations. An atomic model which requires a sufficiently large supercell for characterization of the highly disordered lattice occupation of multi-principal elements is beyond the ability of DFT-based computational calculation methods.^[54] The continuously growing computational power has significantly increased the predictive power of theoretical calculations. Significant advances and evolution in simulation methods and computational science occurred in the last decades, resulting in the rapidly increasing computational capacity.^[55] The big data approaches, including high-throughput virtual screening and machine learning, will support dealing with extensively large databases, uncover complexities, and design novel materials with enhanced properties.^[56] In HEMs, predictions have been studied mainly for HEAs.

HEAs' rational design and controllable synthesis in a virtually unlimited compositional space remain a challenge. As reported by Yao et al., a series of multi-elemental alloy nanoparticles (MEA-NPs) as highly active and robust catalysts were first predicated using the computationally aided, entropy-driven calculations and then synthesized through the high-temperature method.^[57] The computational strategy involved prescreening millions of compositions, in which DFT calculations were used to predict the alloy formation, and a hybrid Monte Carlo and molecular dynamics method were applied to examine the structural stability. Figure 3a–c illustrates the formation of ternary,

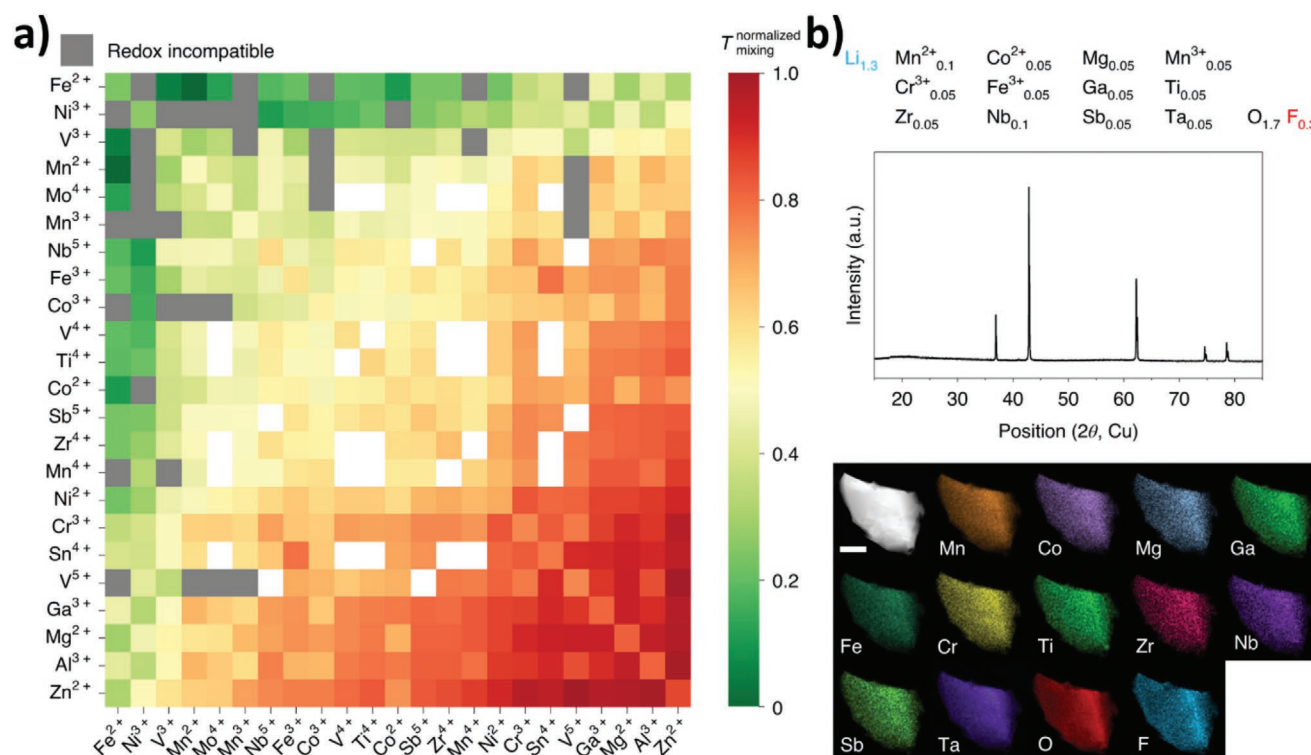


Figure 2. Density functional theory guided HE DRX cathode design. a) The quantified compatibility of different transition metal pairs with a normalized scale between 0 (highly compatible) and 1 (not compatible). The grey fields represent redox incompatible couples. The white squares indicate transition metal couples that were not included. b) HE DRX containing 12 cationic species with pure rock-salt phase confirmed by XRD pattern (top) and homogeneous element distribution demonstrated by STEM/EDS mapping (bottom). Scale bar: 400 nm. Reproduced with permission.^[29] Copyright 2021, Springer Nature.

quaternary, and quinary alloys, in which ten principal elements including Ru, Rh, Ir, Pd, Cr, Fe, Co, Ni, Cu, and Mo are considered, with the constitutions of each element varying from 5% to 50%, with a step size of 5%. For the ternary alloys, 7740 compositions are derived from these ten active elements, of which ≈61% (a statistical data) are single-phase alloys (represented by yellow dots), while the others are not single-phase solid solution (represented by purple dots). In the case of a quinary system with more elements involved, a total number of more than 7 million compositions are screened, with an increased ratio (Figure 3d) of solid solution alloy phase, which indicates the entropy-driven single-phase stabilization. High-temperature synthesis through electrical Joule heating is carried out, and the computational predictions are realized experimentally. As depicted in Figure 3e,f, the experimentally obtained quinary MEA-NPs show thermal stability up to 600 °C from room temperature. The high-temperature catalytic functionality is demonstrated for NH₃ decomposition. As demonstrated in this work, this computationally aided methodology shows the capability of the calculations to predict both alloy and nonalloy formation, which guides the synthesis direction for the possible compositions that could give rise to solid solution alloy phases well before experimental.

HEAs are receiving more and more attention, and the production of experimental data has been dramatically accelerated, making the large-scale databases of structures and properties of chemical compositions and crystal structures available.^[55,58]

The turning of computational chemistry and material science to machine learning, which is steering research into a new data-driven science paradigm, is coming at the right time. In the age of big data, the demands for machine learning and other computationally added approaches are drastically growing in phase and structure prediction and synthesis of HEAs. As a branch of artificial intelligence, machine learning offers new approaches to boost discovering new materials, mapping the connection of targeted property to numerous materials descriptors. Machine learning aims to create statistical models for data analysis and make accurate predictions through developing algorithms that should learn by themselves based on the available data. It is anticipated that machine learning will help identify single-phase solid solution compositions from the vast compositional space. Other computationally aided calculations, including high-throughput first-principles investigations, are also reported for conventional material for energy-related applications.^[59] These high-throughput computational design has demonstrated its promising predicting ability, which will play an essential role in developing HEMs for energy-related applications.

Supervised machine learning combined DFT calculations have demonstrated the predictive ability to optimize HEAs as CO₂ and CO reduction reactions catalysts by scanning massive spaces of HEAs while aiming at a chance for suitable catalysts. Pedersen et al. discovered the adsorption energies for CO and H on the disordered HEAs (111) surface with the presumption

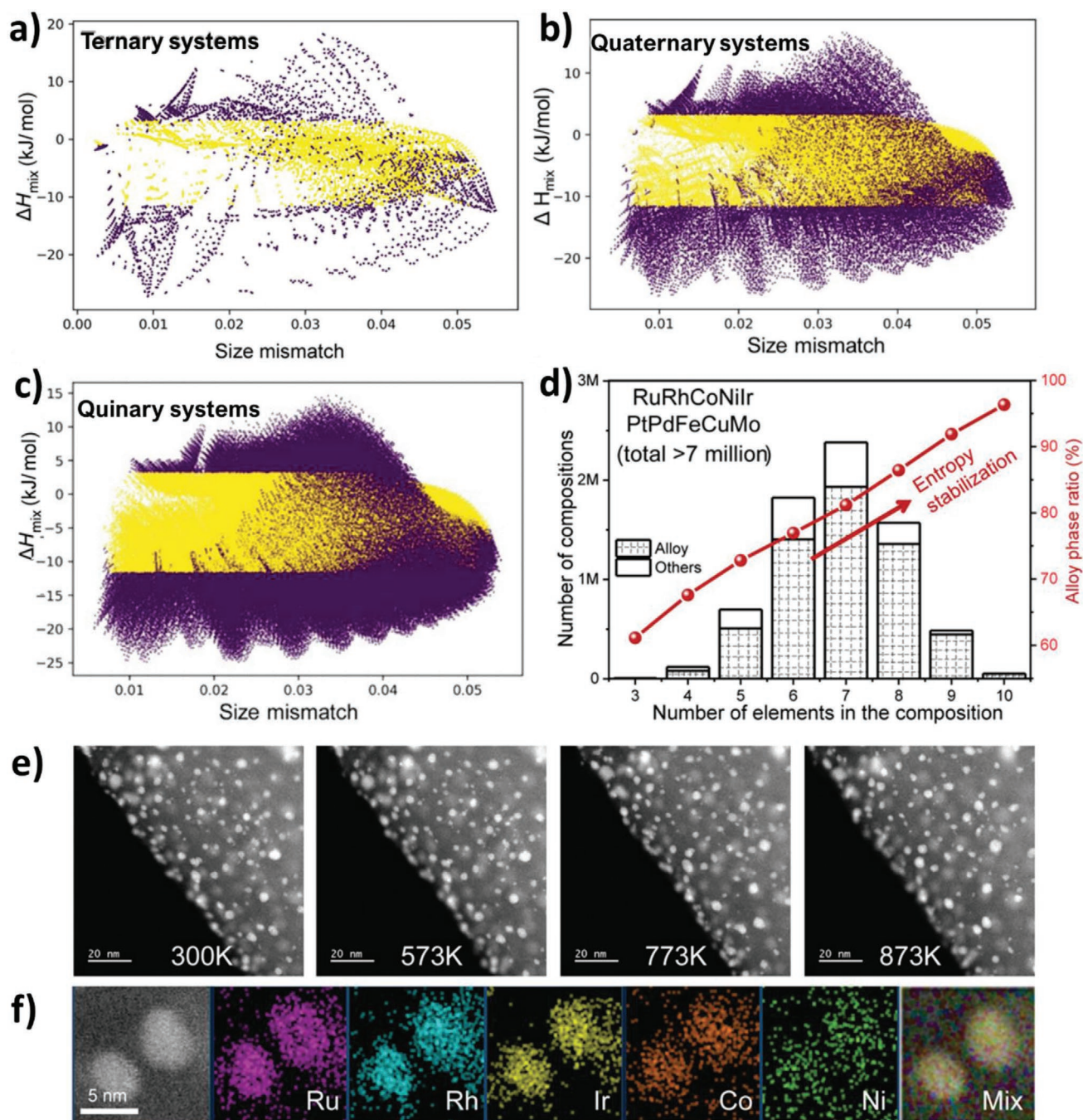


Figure 3. Multi-elemental alloy nanoparticles (MEA-NP) composition screening, prediction, and synthesis. Phase selection diagrams for a) ternary, b) quaternary, and c) quinary MEA-NPs made from the 10 catalytically active elements (Ru, Rh, Ir, Pd, Cr, Fe, Co, Ni, Cu, and Mo, with the constitutions of each element varying from 5% to 50% with a step size of 5%). Yellow dots represent single-phase solid solution, while purple dots represent no single-phase. d) Numbers of the compositions (left) and the ratio of the alloy phase in these compositions (right) as a function of the multi-elemental systems. e) In situ thermal stability of Ru-5 MEA-NPs from room temperature up to 600 °C (held at each temperature for over 30 min). f) Corresponding EDS mapping after the in situ stability test, showing a uniform alloy structure. Reproduced with permission.^[57] Copyright 2020, American Association for the Advancement of Science.

that the adsorption energy is exclusively determined by the elemental labels and locations relative to all adsorbate atoms (Figure 4). Because of the disordering, different microstructures of the adsorption site are present (Figure 4a), determining different adsorption features of the reaction intermediates. Spe-

cifically, the weak hydrogen (H) adsorption and strong carbon monoxide (CO) adsorption are considered essential. Figure 4b shows the differences of the CO and H adsorption energies obtained from DFT calculations and Gaussian process regression predictions for fcc HEAs CoCuGaNiZn and AgAuCuPdPt.

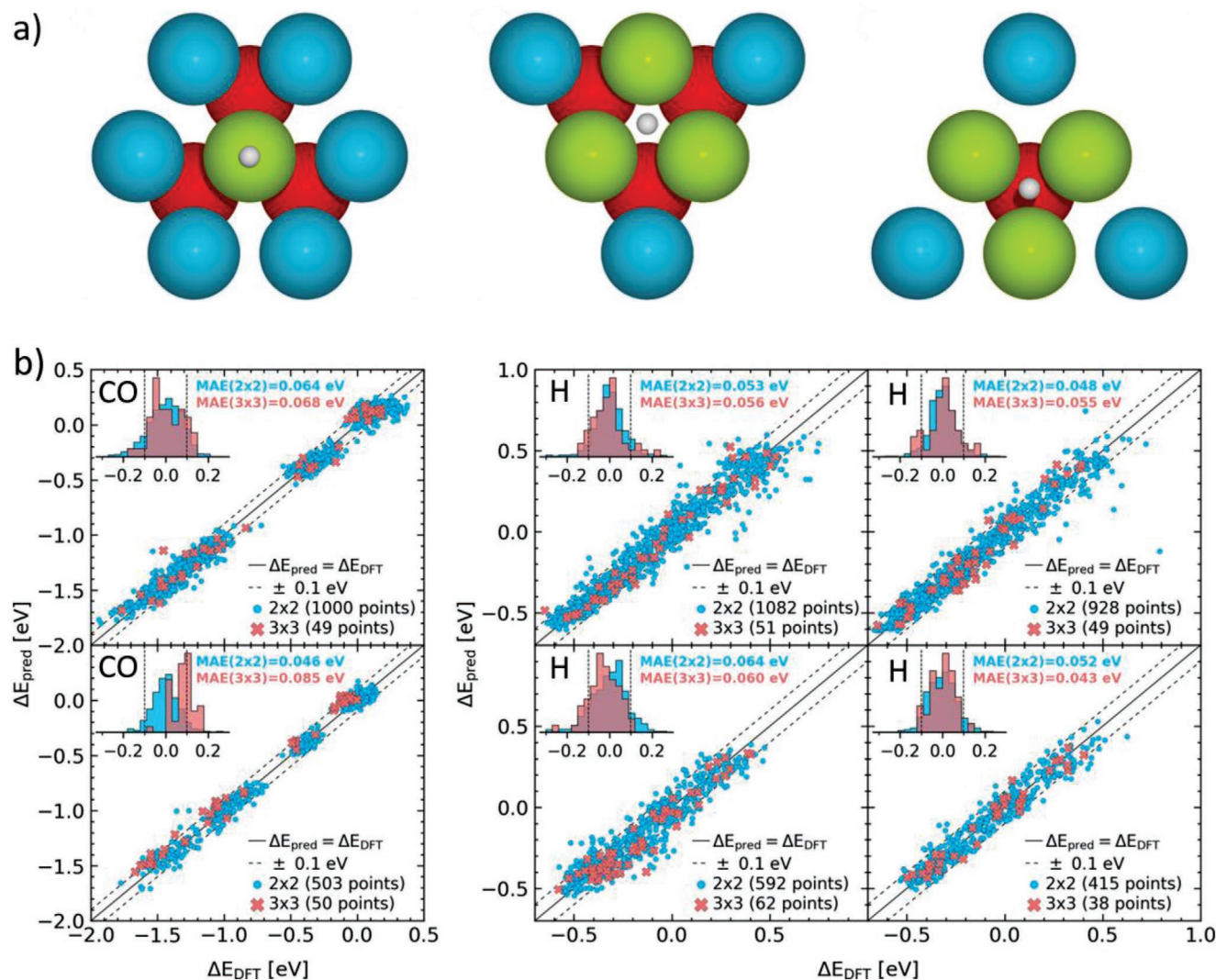


Figure 4. Density functional theory with supervised machine learning calculations of HEAs for catalysis. a) Surface configurations around the adsorption site on a (111) surface, including on-top, FCC-hollow, HCP-hollow adsorption, and adsorbing intermediate, are represented by white circles. b) Upper corresponds to CoCuGaNiZn and bottom to AgAuCuPdPt. Predicted (ΔE_{pred}) versus calculated (ΔE_{DFT}) adsorption energies of on-top CO, fcc-hollow H, and hcp-hollow H. Blue and red indicate data for 2×2 atoms slabs and 3×3 atoms slabs, respectively. Prediction errors (defined as $\Delta E_{\text{pred}} - \Delta E_{\text{DFT}}$, in eV) are shown in insets. Reproduced with permission.^[91] Copyright 2020, American Chemical Society.

The adsorption energies predicted by Gaussian process regression are within the accepted error range equal to a deviation of ± 0.1 eV (dashed lines). Therefore, theoretical calculations of DFT with supervised machine learning provide a promising capability for predicting effective catalyst candidates even lack beforehand knowledge of their catalytic properties and offer an approach to optimize the composition of HEAs with optimal catalytic performance.

As guidance in searching for candidate materials exhibiting target properties, computational science complements this effort to narrow the search space. Material with predicated potentially good performance needs to be synthesized for real-world applications. Especially for energy storage and conversion applications, material syntheses need to be performed on a vast scale requiring reproducibility, safety, and environmentally friendly processes. Therefore, the continuing speed-up

in computing prediction capabilities needs to be paralleled by increased experimental throughput. A new paradigm of the future approach would be combining computational prediction and high-throughput experimental methods efficiently. High-throughput computational techniques have been introduced for discovering new ternary oxides.^[60] A combination of machine learning was applied to first extract “chemical rules” from an experimentally available crystal structure database, suggesting new compositions and structures candidates. Ab initio computation was further used to examine the candidate list with an accurate energy model, predicting 209 new compounds. Although the computational method can efficiently accelerate the discovery/prediction of potential new compounds, the challenges/limitations exist for the experimental proof, which also needs to be carried out efficiently, for example, high-throughput experimental. Conversely, the most common limiting factor in

machine learning applications to material science is acquiring enough data for reliable parameterization.^[61] High-throughput experimental provides a powerful method for creating a massive amount of raw data, in which knowledge and insights can be extracted by machine learning.

4. High-Throughput

Investigating multi-component systems composed of three or more elements with a desired structure and properties is very challenging. Traditionally, the development of new materials is generated from a single experiment (“trial and error” and “directed research”) at a time; this process results in high cost, long manufacturing and analysis time, and exponential growth as the complexity of the material increases. However, the vast compositional space of multi-component systems, such as HEMs, hinders selecting suitable material candidates for many different applications.^[7,8,10,62] Therefore, significant efforts have been dedicated to developing combinatorial synthesis approaches (aided by artificial intelligence) and theoretical predictions to hunt specific materials of interest for industry and academic research.^[63,64–69] A synergy among experimental, theoretical predictions, and artificial intelligence will significantly aid the development of multi-component materials for targeted properties. A common trend in the workflows^[64,67,69–72] presented in different fields suggests a path toward developing autonomous and automated protocols, as depicted in **Figure 5**. The workflow starts with combinatorial synthesis methods, automated characterization techniques (with or without a feedback-measuring loop), automated data analysis, creating a material database or material library, and selecting materials of interest. The complete workflow can be closed by selecting samples of interest for further synthesis and characterizations.^[73] However, without theoretical predictions or computational approaches, the workflow can be considered a fast “trial and error” approach.

The relevance of the workflow is that it has been successfully implemented in different fields, leading to a high amount of data that can be used appropriately for targeted properties. Due to the vast chemical compositional space offered by multi-component materials (such as HEOs), a workflow depicted in **Figure 5** will enormously aid in investigating HEOs for energy-related applications. For instance, following such an approach, it was possible to screen a vast compositional space for an HEO and present a material library relating chemical composition, crystal structure, and the bandgap.^[69] Thus, research experience for element choice and theoretical predictions combined with high-throughput and artificial intelligence will accelerate the discovery of promising materials.

Several combinatorial studies using high-throughput have been conducted to explore the vast compositional space of organic–inorganic perovskites,^[10,15–17,20] organic materials,^[21–25] and multi-component materials.^[65,67,72,74,75] In the case of HEOs (systems containing at least five cations), there is, up to date, one high-throughput study reported in the literature.^[69] Therefore, in the following sections, the literature review is limited to some exemplary studies (conducted on ternary/quaternary systems, organic–inorganic, and organic materials) that can be adapted to develop high-throughput studies on HEOs.

Based on solid-state reactions or wet chemistry methods, HEOs have been fabricated (via “trial and error”).^[14,76] There are several advances in the automated synthesis using wet chemistry, such as the fabrication of organic–inorganic perovskites and organic materials.^[68,71,77] In these studies, the synthesis process is conducted using liquid handling robotics, which allows the combination of several water-based solutions and can vary the volume of each solution (similar to doping). This process is analogous to the “trial and error” synthesis of HEOs using reverse co-precipitation and, to a lesser extent, to nebulized spray pyrolysis, flame spray pyrolysis, and spin coating.^[14,76] The liquid handling robotic technology can be adjusted to prepare

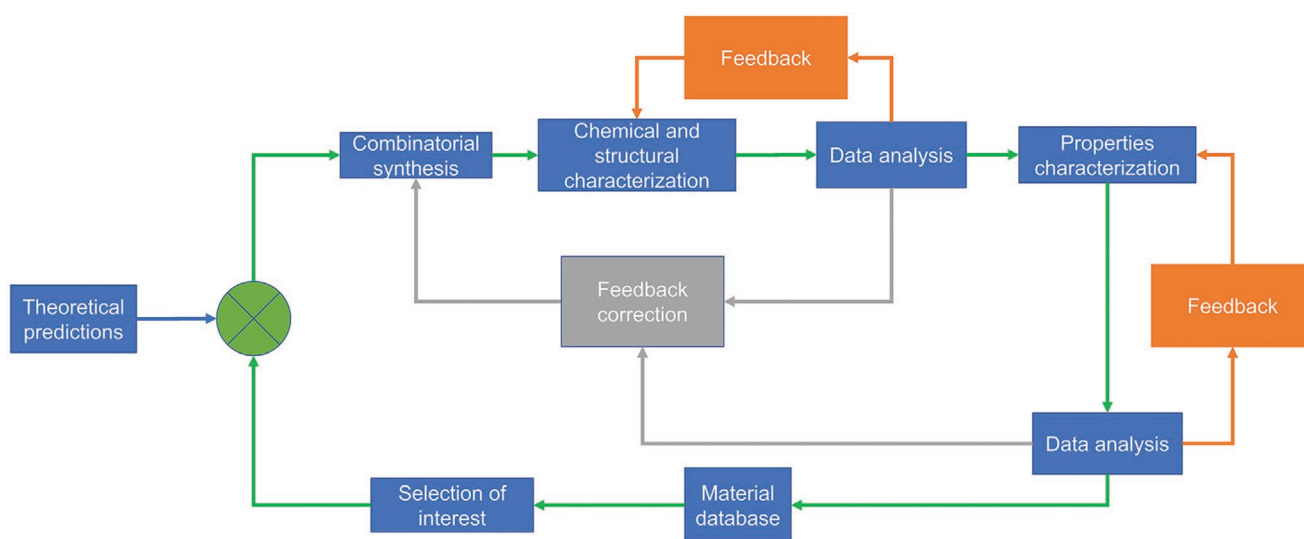


Figure 5. Workflow. Left: workflow paradigm similar to “trial and error” coupled with theoretical predictions. Right: closed-loop discovery utilizing inverse design and a tightly integrated workflow to enable faster identification, scale-up, and manufacturing. Feedback loops during characterization can provide instructive information to correct the measuring method or adjust the synthesis method, leading to a more autonomous workflow.

hundreds of different solutions containing different volumes to vary the chemical composition of the desired material or to produce combinatorial studies of several candidate elements.^[69] As described in the organic–inorganic perovskites study by Li et al.,^[68] the resulting mixed solutions were not exposed to temperatures exceeding 105 °C, which are insufficient for the synthesis calcination process of HEOs (>700 °C) using wet chemistry. Therefore, such high-throughput synthesis protocols for the synthesis of HEOs require technical modifications. One example is the low thermal mass reactor device designed by Chan et al.,^[78] which raises the temperature during colloidal nanocrystals' synthesis (using a liquid handling robotic system) to 350 °C. Similarly, the produced solutions can be incorporated into an automated spin coating device, as developed by Macleod et al.,^[79] however, the additional calcination process required for the HEOs needs to be implemented.

A facile method developed for wet chemistry methods shows that it is possible to build up to 100 compositional arrays with temperature control (up to 250 °C).^[80] One promising approach proposed by Matsubara et al.^[81] adds an extra step during the synthesis using liquid handling robotics. In this approach, the liquid solutions in the desired quantities are transferred into alumina plates, which can withstand high temperatures.

Similarly, quartz plates were used for the calcination process of HEOs.^[69] For solid-state reactions synthesis, the work conducted by Shuang et al.^[82] shows an automated, flexible way to fabricate bulk ceramics via precise volume controlling of powder materials. Song et al.^[83] prepared 91 samples by dosing the amounts of ceramic powders to be combined, although each of the samples has to be transferred manually to molds for isostatic pressing. Using powder dosing units, Stegk et al.^[84] fabricated up to 40 samples in parallel of the binary material system $\text{ZrO}_2\text{--Y}_2\text{O}_3$.

The studies mentioned above provide insightful engineered solutions that are crucial for developing a fully automated synthesis-characterization workflow. The production of HEOs films via vapor deposition is still in its early stages. However, successful high-throughput approaches using vapor deposition have been implemented for multi-component systems (up to 4 components) and HEAs.^[66,72,75,81,84–88] Therefore, these synthesis paths can provide rightful approaches that can overcome further difficulties in developing a fully automated synthesis process for HEOs. **Figure 6** visualizes different synthesis techniques that can be potentially used to fabricate HEOs. Figure 6a shows a promising approach that uses automated procedures (via liquid handling robotics) for pouring liquid precursor

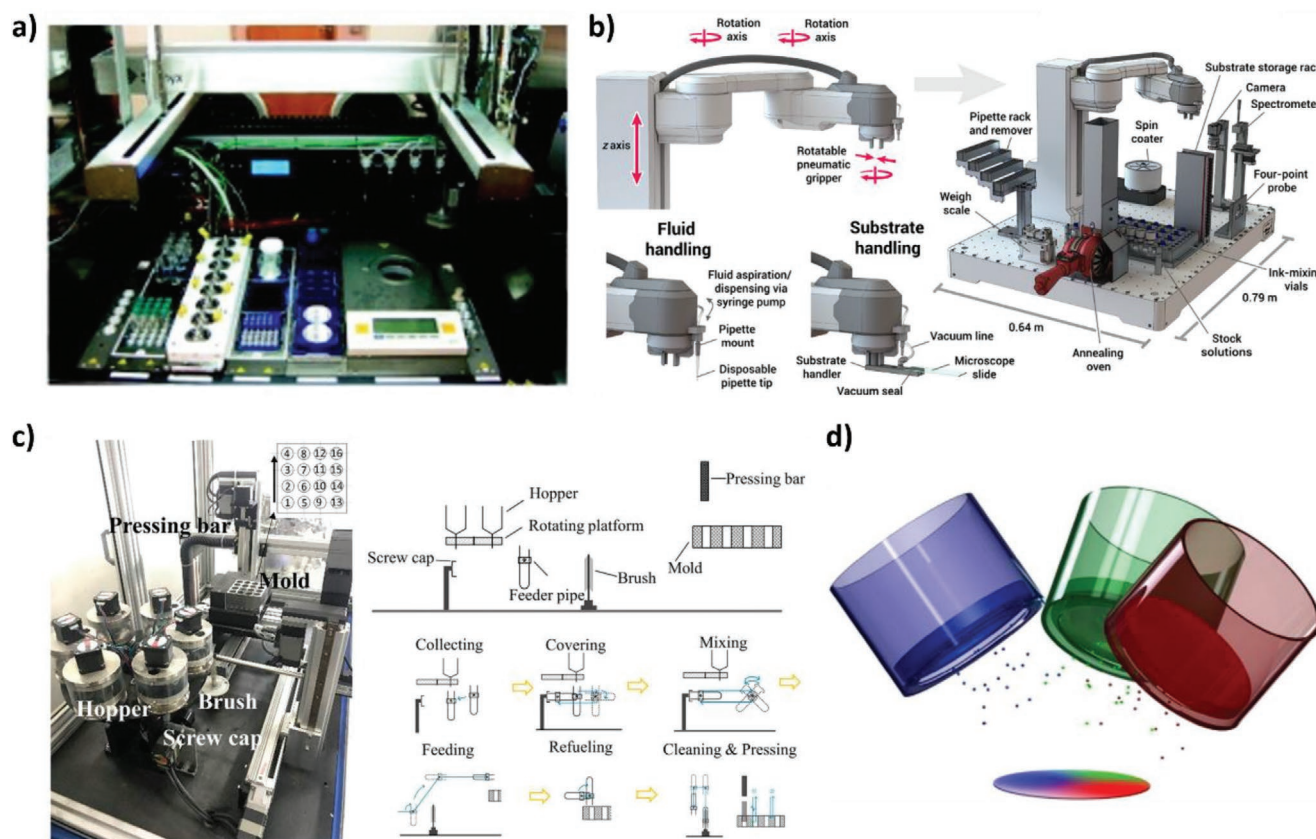


Figure 6. High-throughput combinatorial synthesis for multi-component systems. a) A workstation for liquid handling robotics used to synthesize colloidal nanocrystals. Reproduced with permission.^[78] Copyright 2010, American Chemical Society. b) Robotic platform designed to synthesize thin films via spin coating, including an annealing oven. Reproduced with permission.^[79] Copyright 2020, American Association for the Advancement of Science. c) An automated platform that allows fabrication of ceramic pellets. Reproduced with permission.^[82] Copyright 2019, AIP publishing. d) Representation of the co-deposition of multiple elements using physical vapor deposition. Reproduced with permission.^[65] Copyright 2012, Elsevier B.V.

materials that allow the fabrication of different materials, for instance, colloidal nanocrystals,^[78] and recently for HEOs (e.g., reverse co-precipitation procedures).^[69] It is demonstrated that by precisely controlling the reaction conditions, this high-throughput method allows to tailor and tune chemical compositions (e.g., the process of doping a material), leading to effective optimization of physical properties concerning specific applications. Another example of using a robotic platform to accelerate synthesis processing is displayed in Figure 6b. The materials precursors are used to fabricate thin films via spin coating, the automated platform is capable of transporting the samples into an annealing furnace, and it is coupled to a module to record the optical spectra of each produced sample. The automated platform in Figure 6b is a self-driving laboratory^[79] and should be considered as an example to follow as a fully automated fabrication process. A critical aspect for properly characterizing ceramic materials is their bulk density (e.g., sintered pellets free of pores and dense films). Highly dense ceramic pellets are desired for studying mechanical or transport (e.g., ionic conductivity) properties, and hence many energy-related applications. In Figure 6c, an automated platform was designed to fabricate ceramic pellets.^[82] Although it is not guaranteed that the density of all such pellets is very high, it will be possible to screen promising candidates and focus on specific chemical compositions. Another way to produce dense materials is the fabrication of films or coatings, as shown in Figure 6d, a representation of the co-deposition of three different elements using magnetron sputtering is depicted.^[65] Using this configuration makes it possible to resolve the spatial chemical composition of the material and analyze gradients in the chemical composition. The drawback of film production via magnetron sputtering, is that the number of elements that are co-deposited is limited by the amount of target materials that can be physically placed inside the equipment.

Two key parameters essential for HEO materials are i) the distribution of the constituent elements should be homogeneous and randomly distributed, and ii) the material should display a single phase.^[18,89] Basic characterization techniques have been used to screen HEOs' chemical composition and crystal structure via scanning electron microscopy coupled with energy-dispersive X-ray spectroscopy (SEM-EDS) and X-ray diffraction (XRD).^[18,39,90] In addition, advanced characterization techniques such as transmission electron microscopy, atom probe tomography, inductively coupled plasma-optical emission spectroscopy, and synchrotron radiation have been utilized to further address the cation distribution in the crystal structure and purity of the crystal structure.^[14,18,39,90]

In the field of inorganic materials, automated characterization using XRD, SEM-EDS, and synchrotron radiation techniques have been developed to screen the basic characteristics of multi-component bulk materials or thin films.^[66,72,75,85–87] Although automated synchrotron radiation experiments can be considered the fastest way to screen the crystal structure of multiple samples, it is limited by beam-time availability. Despite the time constraints and big data analysis (which can be aided by artificial intelligence), the relevance of automated characterization is enforced by developing materials libraries, which are helpful for the fast identification of materials functionalities of interest. For instance, high-throughput studies

of shape memory alloys based on the compositional space of the quaternary Ni–Ti–Cu–V showed that out of 177 different compositions, 32 displayed a shape memory effect.^[87] In the case of oxides, high-throughput studies on ternary metal vanadate ($M-V-O$, $M=Cu, Ag, W, Cr, Co, Fe$) allow correlating the microstructural and chemical features of the oxides with their possible functionality in solar water splitting.^[86] Using a scanning superconducting quantum interference device microscope, Hasegawa et al. built a magnetic material library for the $La_{1-x}Ca_xMnO_3$ and $Nd_{1-x}Sr_xMnO_3$ films.^[92] The automation of an ultraviolet–visible spectrometer allowed to conduct band gap measurements on a series of samples, which deviate chemically from equiatomic HEOs.^[69]

Figure 7 displays three examples of material libraries for binary, quaternary, and quinary oxides. The main idea of the material library is to provide a visual correlation of chemical composition, crystal structure, and an investigated property. In Figure 7a, a material library correlating the bandgap and the photocurrent density of the Fe–V–O combinatorial thin film was presented by Kumary et al., highlighting that between 54 and 66 at% Fe the maximum photocurrent density is achieved, the material was obtained by using magnetron sputtering.^[87] Matsubara et al. evaluated the ionic conductivity in the Ca–(Nb,Ta)–Bi–O system, for which 288 compositions were fabricated. As depicted in Figure 7b, the material library provides a practical approach to visualizing the fabricated samples' ionic transport properties.^[81]

In Figure 7c–e, landscapes of the crystal structure, oxygen vacancy concentration, and bandgap allow visualizing the effect of 91 samples that chemically deviate from the equiatomic (located in the center of the diagrams) HEO ($CeLaSmPrY$)O₂.^[69] These landscapes show, for instance, that the majority of the samples tend to form a fluorite crystal structure. Meanwhile, the oxygen vacancy concentration and bandgap maps provide information to select a region of interest; for example, the maps allow finding which chemical compositions are needed if a material with a single-phase, low vacancy concentration, and low bandgap is desired. The visualizations mentioned above, presented in Figure 7, can facilitate compositional selection based on basic parameters or properties, for example, a specific ionic conductivity, bandgap, or the correlation between the desired crystal structure and property. It is noteworthy that the materials libraries presented in Figure 7 can be considered as isothermal phase-property diagrams since no extra heat treatments were made on the produced samples. This means that, for each additional heat treatment, a new material library will be generated.

In powders, like most of the HEOs, the characterization process requires human interaction, that is, removing the sample from typically a ceramic crucible (necessary for high-temperature calcination processes) to a device that can realize the measuring. The automation of characterization techniques depends on the status of the as-synthesized samples. For example, samples produced via magnetron sputtering (like in Figure 6d) can be easily set on automated X-ray diffraction analysis. In contrast, in the case of powders, the X-ray diffraction experiment can require further engineer solutions (modification of synthesis processing). Indeed, a compatibility technically engineered solution must be designed for each

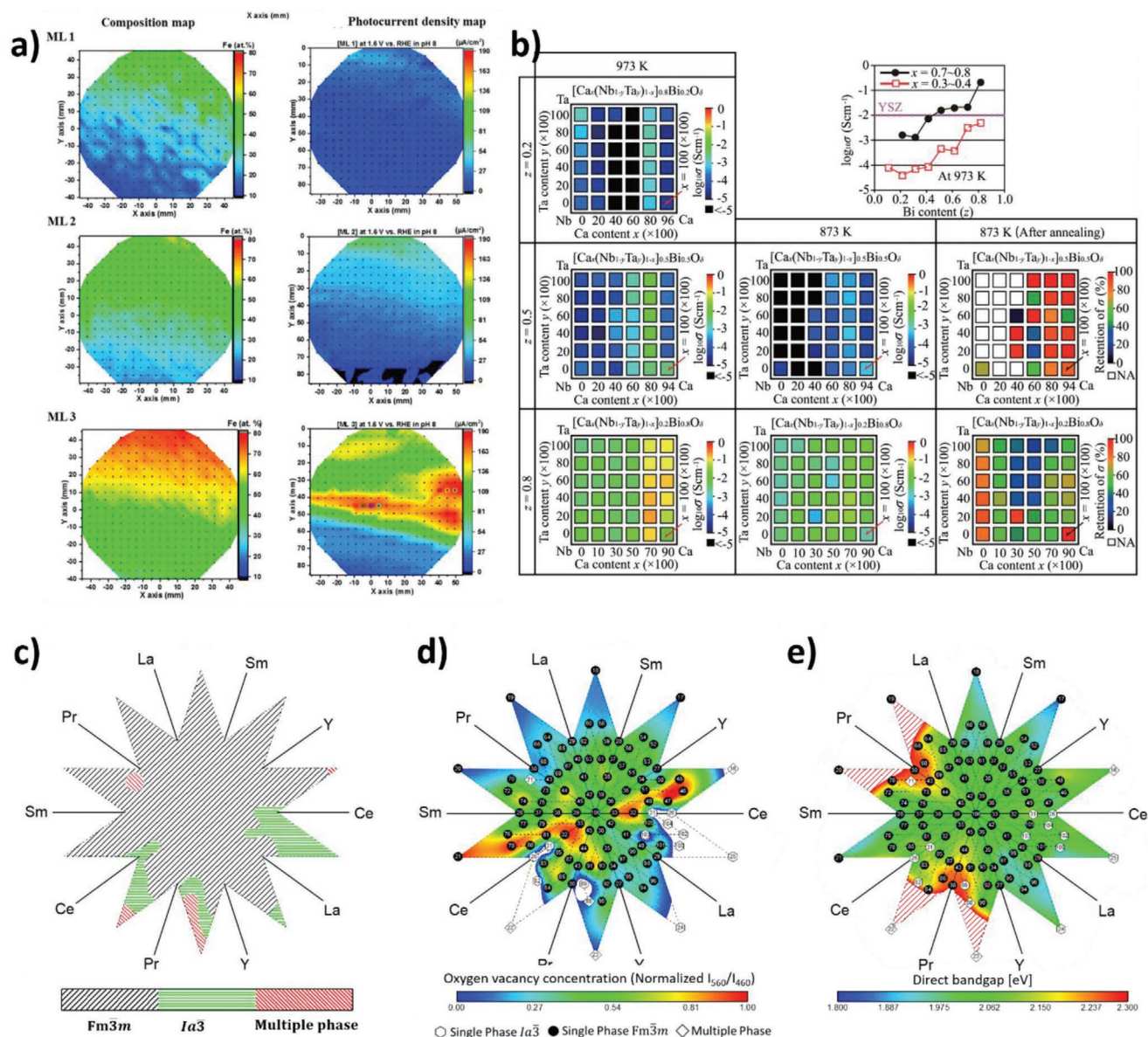


Figure 7. Materials libraries for multi-component oxides. a) Material libraries obtained via physical vapor deposition. ML1, ML2, and ML3 were obtained with different deposition conditions; the chemical composition maps show the variation of Fe content for each deposition condition, while the photocurrent density map highlights that between 54 and 64 at% Fe the highest photocurrent densities were found (ML3 maps). Reproduced with permission.^[87] Copyright 2018, American Chemical Society. b) Chemical composition and ionic conductivity maps for the quaternary system $\text{Ca}(\text{Nb,Ta})\text{Bi-O}$. Reproduced with permission.^[81] Copyright 2020, Springer Nature. c) Crystallographic phase map, d) landscape of the oxygen vacancy concentration (I_{560}/I_{460}), and e) phase property diagram (direct bandgap) for the chemical space of 91 oxides containing three or more elements of the HEO (CeLaSmPrY) O_2 . Reproduced with permission.^[69] Copyright 2021, Wiley-VCH GmbH.

synthesis process to avoid human interaction and facilitate automated characterization measurements. In high-throughput experimental studies, the choices of elements or compositional ranges are based on research experience or predictions from theoretical simulations. The common trend is that experimental high-throughput must be developed in combination with computational-theoretical design.

High-throughput techniques can be classified regarding their targeted scopes. Upscaling processes might not be that

important for material exploration since today many characterization techniques require only a small amount of material. Indeed, producing larger quantities of materials might be a bottleneck of this technology; for example, high-throughput techniques presented in Figure 6a,b can produce only small amounts of materials. Although many synthesis techniques allow increasing the amount of produced sample without great additional efforts (e.g., a robot filling more mL or L of liquids into vials combined with a solid-state synthesis in

a large furnace), other conventional synthesis methods for ceramics, like self-propagating high-temperature synthesis that scales with the amount of reactants, are not so much suitable for high-throughput synthesis method. Therefore, the big strength at present of the high-throughput methods is the fast production of many different samples, for example, in a recent work, the authors claim synthesis and characterization of ≈ 100 samples in 1 week, but each sample only contains material in the milligram range.^[69] As for the introduction of many other upscaling processes in different fields of science, a general adaptation or adjustment of the existing synthesis procedures has to be performed to suit the requirements of high-throughput techniques, with the possible consequence of abandoning some conventional techniques. Nevertheless, techniques like solid-state synthesis, nebulized spray pyrolysis, and physical vapor deposition are very suitable for high-throughput methods and allow the development of promising experiments. In this regard, high-throughput techniques are more suited for materials exploration than for large-scale synthesis. Following, upscaling production of the candidate material can be conducted using industrial equipment.

Another bottleneck that appears especially toward the goal of the rational and computational design of high-throughput experiments is that a parallel synthesis can be conducted or implemented easily. Still, the characterization often has to be performed in a serial way (for example, X-ray diffraction). This change from a parallel to many serial experiments, especially the lack of parallel characterizations, enlarges the time factor necessary to perform the whole high-throughput/machine learning/computational design cycle. Due to the large time factor, less information can be collected for the machine learning process, and the information needed for the computational design are gathered slowly. In this regard, scientific, and most importantly, engineering efforts, to enable the parallel characterization of materials, need to be developed to provide the necessary information in a reasonable time scale for machine learning and, subsequently, the computational design. The computational design will be positively enhanced if the whole cycle (as in the workflow in Figure 5) is accelerated and the information generation increases exponentially.

5. Outlook

Due to their extraordinary mechanical, physical, chemical, and electrochemical properties, high-entropy materials, including high-entropy alloys and high-entropy ceramics with a constitution in equal or near-equal molarity, have been intensively investigated in different fields. Our review has highlighted in particular energy-relation properties and applications. Until now, the research on compositions, structures, and properties of high-entropy materials has remained mainly based on experiments through “trial and error” or “directed research” approaches. The computational design and high-throughput are just beginning to play a role. Based on the experiments, theoretical calculations would serve as an effective approach to clarify the relationship between the structures, composition, and properties and streamline material innovation.

Over the past decades, computational-driven materials design has gained an increasingly predictive capacity with the advancement of computer hardware and software and is playing a significant role in accelerating the discovery of cost-effective materials. The continuous increase of computational resources and the development of more efficient codes enable computational high-throughput studies. However, high-throughput computational simulation for high-entropy materials might face the prediction challenge for developing codes with complex multiscale models that are truly predictive. Yet, the computational power needed to feed a large scale of highly accurate data from first-principles calculations is still the bottleneck. Machine learning, which can go far beyond the limitations of the current electronic structure method, seems to be a more appropriate computational technique, allowing the investigation of novel complex material systems with emerging phenomena. The challenges exist in acquiring the enormous amount of data and assuring the quality of the training data, which highly determine the accuracy of the machine learning model.

High-throughput experimental can rapidly establish the material “libraries” that correlate the chemical composition and crystal structure with functional properties, which is particularly appropriate to the experimental complement of computational calculation and simulation. Computational design coupled with high-throughput and artificial intelligence seems not far to be a reality in the laboratory, where the production and characterization of many different samples can be freely conducted, and failure is more tolerated. However, the high-throughput synthesis methods of choice or computational predictions may not be fully adjusted to industry requirements. For example, using liquid handling robotics, it is possible to synthesize ≈ 100 samples in several days. However, the amount of sample is low (hundreds of milligram), which is by far out of industrial scalability. In this context, automated high-throughput laboratories can be the place for selecting candidate materials, for which further development must be conducted for their scalability. Further assessment for applications and commercialization will benefit from implementing them together with industrial collaborations, which can be considered a further feedback loop for checking the lab research’s insufficiencies and optimizing the research to fit the real-world condition of an application.

From the perspective of the future development of high-entropy energy materials, computational approaches like density functional theory and machine learning need to be further implemented in the research of high-entropy ceramics other than high-entropy alloys. In contrast to the extensive computational investigation of high-entropy alloys as electrocatalysts, high-entropy ceramics, which have found their electrocatalytic applications for the oxygen evolution reaction, deserve much attention and effort to further expand their energy conversion applications. Like the emergence of big-data-driven materials informatics, interdisciplinary collaborations will bring other breakthrough applications to overcome many bottlenecks encountered by conventional materials.

Further combining experiments and computational simulations, especially high-throughput computational analyses and high-throughput experimental, will allow researchers to explore the phase and complex compositional space of high-entropy materials more efficiently while cutting the time and cost of

material design substantially. Predictive material research, thereby, serves as a fast track toward discovery and innovation. Moreover, functional characteristics of high-entropy materials are also connected with microstructure, surface condition, and interface constructions. High-throughput computations as machine learning could be trained based on a vast experimental database for the requirement like microstructure or morphology. Other facile and rapid processes like high-throughput synthesis and electrochemical techniques require more investment and efforts to accelerate the identification of the materials of functional application. A combination of both will promote the development and application of high-entropy materials in energy storage and conversion. This particularly applies to fast-tracking innovation in the field of novel materials with complex composition, such as the emerging material class of MXene.

Acknowledgements

V.P. acknowledges the funding of the DigiBatMat project (03XP0367A) within the competence cluster for battery cell production (ProZell) by the Federal Ministry of Education and Research (Bundesministerium für Bildung und Forschung). B.B. acknowledges the support from EnABLES and EPISTORE, projects funded by the European Union's Horizon 2020 research and innovation program under Grant Agreement Nos. 730957 and 101017709, respectively. B.B. also acknowledges funding from the Kera-Solar project (Carl Zeiss Foundation). Q.W. and V.P. thank Eduard Arzt (INM) for his continued support.

Open access funding enabled and organized by Projekt DEAL.

Conflict of Interest

The authors declare no conflict of interest.

Keywords

computational design, high-entropy materials, high-throughput, trial and error

Received: August 2, 2021

Revised: September 30, 2021

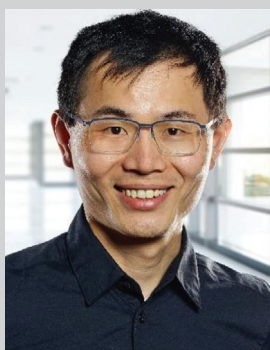
Published online: October 31, 2021

- [1] J.-M. Tarascon, S. Haroche, J.-M. Tarascon, *Chemistry of Materials and Energy. Examples and Future of a Millennial Science*, Collège de France, Paris 2017.
- [2] A. Manthiram, *Nat. Commun.* **2020**, *11*, 1550.
- [3] a) M. Naguib, M. Kurtoglu, V. Presser, J. Lu, J. Niu, M. Heon, L. Hultman, Y. Gogotsi, M. W. Barsoum, *Adv. Mater.* **2011**, *23*, 4248; b) M. Naguib, O. Mashtalir, J. Carle, V. Presser, J. Lu, L. Hultman, Y. Gogotsi, M. W. Barsoum, *ACS Nano* **2012**, *6*, 1322.
- [4] B. Anasori, M. R. Lukatskaya, Y. Gogotsi, *Nat. Rev. Mater.* **2017**, *2*, 16098.
- [5] M. Han, K. Maleski, C. E. Shuck, Y. Yang, J. T. Glazar, A. C. Foucher, K. Hantanasirisakul, A. Sarycheva, N. C. Frey, S. J. May, V. B. Shenoy, E. A. Stach, Y. Gogotsi, *J. Am. Chem. Soc.* **2020**, *142*, 19110.
- [6] M. Benchakar, L. Loupias, C. Garnero, T. Bilyk, C. Morais, C. Canaff, N. Guignard, S. Morisset, H. Pazniak, S. Hurand, P. Chartier, J. Pacaud, V. Mauchamp, M. W. Barsoum, A. Habrioux, S. Célérier, *Appl. Surf. Sci.* **2020**, *530*, 147209.

- [7] B. Cantor, I. T. H. Chang, P. Knight, A. J. B. Vincent, *Mater. Sci. Eng., A* **2004**, *375–377*, 213.
- [8] J. W. Yeh, S. K. Chen, S. J. Lin, J. Y. Gan, T. S. Chin, T. T. Shun, C. H. Tsau, S. Y. Chang, *Adv. Eng. Mater.* **2004**, *6*, 299.
- [9] C. Oses, C. Toher, S. Curtarolo, *Nat. Rev. Mater.* **2020**, *5*, 295.
- [10] D. B. Miracle, O. N. Senkov, *Acta Mater.* **2017**, *122*, 448.
- [11] S. J. McCormack, A. Navrotsky, *Acta Mater.* **2021**, *202*, 1.
- [12] C.-H. Lai, S.-J. Lin, J.-W. Yeh, S.-Y. Chang, *Surf. Coat. Technol.* **2006**, *201*, 3275.
- [13] M. Braic, V. Braic, M. Balaceanu, C. N. Zoita, A. Vladescu, E. Grigore, *Surf. Coat. Technol.* **2010**, *204*, 2010.
- [14] C. M. Rost, E. Sachet, T. Borman, A. Moballegh, E. C. Dickey, D. Hou, J. L. Jones, S. Curtarolo, J.-P. Maria, *Nat. Commun.* **2015**, *6*, 8485.
- [15] a) S. K. Nemani, B. Zhang, B. C. Wyatt, Z. D. Hood, S. Manna, R. Khaledialidusti, W. Hong, M. G. Sternberg, S. Sankaranarayanan, B. Anasori, *ACS Nano* **2021**, *15*, 12815; b) Z. Du, C. Wu, Y. Chen, Z. Cao, R. Hu, Y. Zhang, J. Gu, Y. Cui, H. Chen, Y. Shi, J. Shang, B. Li, S. Yang, *Adv. Mater.* **2021**, *33*, 2101473.
- [16] A. Sarkar, B. Breitung, H. Hahn, *Scr. Mater.* **2020**, *187*, 43.
- [17] a) A. Amiri, R. Shahbazian-Yassar, *J. Mater. Chem. A* **2021**, *9*, 782; b) Y. Chen, H. Fu, Y. Huang, L. Huang, X. Zheng, Y. Dai, Y. Huang, W. Luo, *ACS Mater. Lett.* **2021**, *3*, 160; c) R.-Z. Zhang, M. J. Reece, *J. Mater. Chem. A* **2019**, *7*, 22148; d) B. L. Musicó, D. Gilbert, T. Z. Ward, K. Page, E. George, J. Yan, D. Mandrus, V. Keppens, *APL Mater.* **2020**, *8*, 040912; e) Y. Ma, Y. Ma, Q. Wang, S. Schweidler, M. Botros, T. Fu, H. Hahn, T. Brezesinski, B. Breitung, *Energy Environ. Sci.* **2021**, *14*, 2883; f) B. Sharma, S. Harini, *Mater. Res. Express* **2019**, *6*, 1165d7; g) Z. Jin, J. Lyu, Y.-L. Zhao, H. Li, Z. Chen, X. Lin, G. Xie, X. Liu, J.-J. Kai, H.-J. Qiu, *Chem. Mater.* **2021**, *33*, 1771; h) T. A. A. Batchelor, J. K. Pedersen, S. H. Winther, I. E. Castelli, K. W. Jacobsen, J. Rossmeisl, *Joule* **2019**, *3*, 834.
- [18] A. Sarkar, Q. Wang, A. Schiele, M. R. Chellali, S. S. Bhattacharya, D. Wang, T. Brezesinski, H. Hahn, L. Velasco, B. Breitung, *Adv. Mater.* **2019**, *31*, 1806236.
- [19] A. Sarkar, L. Velasco, D. Wang, Q. Wang, G. Talasila, L. de Biasi, C. Kübel, T. Brezesinski, S. S. Bhattacharya, H. Hahn, B. Breitung, *Nat. Commun.* **2018**, *9*, 3400.
- [20] Q. Wang, A. Sarkar, D. Wang, L. Velasco, R. Azmi, S. S. Bhattacharya, T. Bergfeldt, A. Düvel, P. Heitjans, T. Brezesinski, H. Hahn, B. Breitung, *Energy Environ. Sci.* **2019**, *12*, 2433.
- [21] V. M. Goldschmidt, *Naturwissenschaften* **1926**, *14*, 477.
- [22] a) P. Sarker, T. Harrington, C. Toher, C. Oses, M. Samiee, J.-P. Maria, D. W. Brenner, K. S. Vecchio, S. Curtarolo, *Nat. Commun.* **2018**, *9*, 4980; b) T. Jin, X. Sang, R. R. Unocic, R. T. Kinch, X. Liu, J. Hu, H. Liu, S. Dai, *Adv. Mater.* **2018**, *30*, 1707512; c) T. Wang, H. Chen, Z. Yang, J. Liang, S. Dai, *J. Am. Chem. Soc.* **2020**, *142*, 4550; d) P. A. Sukkurji, Y. Cui, S. Lee, K. Wang, R. Azmi, A. Sarkar, S. Indris, S. S. Bhattacharya, R. Kruk, H. Hahn, Q. Wang, M. Botros, B. Breitung, *J. Mater. Chem. A* **2021**, *9*, 8998; e) R.-Z. Zhang, F. Gucci, H. Zhu, K. Chen, M. J. Reece, *Inorg. Chem.* **2018**, *57*, 13027; f) J. Gild, Y. Zhang, T. Harrington, S. Jiang, T. Hu, M. C. Quinn, W. M. Mellor, N. Zhou, K. Vecchio, J. Luo, *Sci. Rep.* **2016**, *6*, 37946; g) Z. Wang, Z.-T. Li, S.-J. Zhao, Z.-G. Wu, *Tungsten* **2021**, *3*, 131; h) X. Zhao, Z. Xue, W. Chen, X. Bai, R. Shi, T. Mu, *J. Mater. Chem. A* **2019**, *7*, 26238; i) Ya. Ma, Yu. Ma, S. L. Dreyer, Q. Wang, K. Wang, D. Goonetilleke, A. Omar, D. Mikhailova, H. Hahn, B. Breitung, T. Brezesinski, *Adv. Mater.* **2021**, *33*, 2101342.
- [23] Y.-F. Kao, S.-K. Chen, J.-H. Sheu, J.-T. Lin, W.-E. Lin, J.-W. Yeh, S.-J. Lin, T.-H. Liou, C.-W. Wang, *Int. J. Hydrogen Energy* **2010**, *35*, 9046.
- [24] a) C.-F. Tsai, P.-W. Wu, P. Lin, C.-G. Chao, K.-Y. Yeh, *Jpn. J. Appl. Phys.* **2008**, *47*, 5755; b) W. Dai, T. Lu, Y. Pan, *J. Power Sources* **2019**, *430*, 104.
- [25] T. Löffler, H. Meyer, A. Savan, P. Wilde, A. Garzón Manjón, Y.-T. Chen, E. Ventosa, C. Scheu, A. Ludwig, W. Schuhmann, *Adv. Energy Mater.* **2018**, *8*, 1802269.

- [26] a) D. Bérardan, S. Franger, D. Dragoe, A. K. Meena, N. Dragoe, *Phys. Status Solidi RRL* **2016**, *10*, 328; b) D. Bérardan, S. Franger, A. K. Meena, N. Dragoe, *J. Mater. Chem. A* **2016**, *4*, 9536.
- [27] N. Osenciat, D. Bérardan, D. Dragoe, B. Léridon, S. Holé, A. K. Meena, S. Franger, N. Dragoe, *J. Am. Ceram. Soc.* **2019**, *102*, 6156.
- [28] a) D. Berardan, A. K. Meena, S. Franger, C. Herrero, N. Dragoe, *J. Alloys Compd.* **2017**, *704*, 693; b) C. Toher, C. Osés, D. Hicks, S. Curtarolo, *npj Comput. Mater.* **2019**, *5*, 69; c) J. Wang, D. Stenzel, R. Azmi, S. Najib, K. Wang, J. Jeong, A. Sarkar, Q. Wang, P. A. Sukkurji, T. Bergfeldt, M. Botros, J. Maibach, H. Hahn, T. Brezesinski, B. Breitung, *Electrochem* **2020**, *1*, 60.
- [29] Z. Lun, B. Ouyang, D.-H. Kwon, Y. Ha, E. E. Foley, T.-Y. Huang, Z. Cai, H. Kim, M. Balasubramanian, Y. Sun, J. Huang, Y. Tian, H. Kim, B. D. McCloskey, W. Yang, R. J. Clément, H. Ji, G. Ceder, *Nat. Mater.* **2021**, *20*, 214.
- [30] Q. Wang, A. Sarkar, Z. Li, Y. Lu, L. Velasco, S. S. Bhattacharya, T. Brezesinski, H. Hahn, B. Breitung, *Electrochem. Commun.* **2019**, *100*, 121.
- [31] N. Qiu, H. Chen, Z. Yang, S. Sun, Y. Wang, Y. Cui, *J. Alloys Compd.* **2019**, *777*, 767.
- [32] E. Lokcu, C. Toparli, M. Anik, *ACS Appl. Mater. Interfaces* **2020**, *12*, 23860.
- [33] H. Chen, N. Qiu, B. Wu, Z. Yang, S. Sun, Y. Wang, *RSC Adv.* **2019**, *9*, 28908.
- [34] a) P. Ghigna, L. Airolidi, M. Fracchia, D. Callegari, U. Anselmi-Tamburini, P. D'Angelo, N. Pianta, R. Ruffo, G. Cibin, D. O. de Souza, E. Quartarone, *ACS Appl. Mater. Interfaces* **2020**, *12*, 50344; b) F. Tavani, M. Fracchia, N. Pianta, P. Ghigna, E. Quartarone, P. D'Angelo, *Chem. Phys. Lett.* **2020**, *760*, 137968; c) B. Breitung, Q. Wang, A. Schiele, Đ. Tripković, A. Sarkar, L. Velasco, D. Wang, S. S. Bhattacharya, H. Hahn, T. Brezesinski, *Batteries Supercaps* **2020**, *3*, 361.
- [35] a) L. Lin, K. Wang, R. Azmi, J. Wang, A. Sarkar, M. Botros, S. Najib, Y. Cui, D. Stenzel, P. Anitha Sukkurji, Q. Wang, H. Hahn, S. Schweidler, B. Breitung, *J. Mater. Sci.* **2020**, *55*, 16879; b) C. Deng, P. Wu, L. Zhu, J. He, D. Tao, L. Lu, M. He, M. Hua, H. Li, W. Zhu, *Appl. Mater. Today* **2020**, *20*, 100680.
- [36] a) H. Chen, N. Qiu, B. Wu, Z. Yang, S. Sun, Y. Wang, *RSC Adv.* **2020**, *10*, 9736; b) T.-Y. Chen, S.-Y. Wang, C.-H. Kuo, S.-C. Huang, M.-H. Lin, C.-H. Li, H.-Y. T. Chen, C.-C. Wang, Y.-F. Liao, C.-C. Lin, Y.-M. Chang, J.-W. Yeh, S.-J. Lin, T.-Y. Chen, H.-Y. Chen, *J. Mater. Chem. A* **2020**, *8*, 21756; c) D. Wang, S. Jiang, C. Duan, J. Mao, Y. Dong, K. Dong, Z. Wang, S. Luo, Y. Liu, X. Qi, *J. Alloys Compd.* **2020**, *844*, 156158; d) H.-Z. Xiang, H.-X. Xie, Y.-X. Chen, H. Zhang, A. Mao, C.-H. Zheng, *J. Mater. Sci.* **2021**, *56*, 8127; e) T. X. Nguyen, J. Patra, J.-K. Chang, J.-M. Ting, *J. Mater. Chem. A* **2020**, *8*, 18963.
- [37] a) J. Arshad, N. K. Janjua, R. Raza, *J. Electrochem. Sci. Technol.* **2021**, *12*, 112; b) L. Y. Tian, Z. Zhang, S. Liu, G. R. Li, X. P. Gao, *Energy Environ. Mater.* **2021**; c) J. Yan, D. Wang, X. Zhang, J. Li, Q. Du, X. Liu, J. Zhang, X. Qi, *J. Mater. Sci.* **2020**, *55*, 6942.
- [38] C. Zhao, F. Ding, Y. Lu, L. Chen, Y.-S. Hu, *Angew. Chem., Int. Ed.* **2020**, *59*, 264.
- [39] J. Wang, Y. Cui, Q. Wang, K. Wang, X. Huang, D. Stenzel, A. Sarkar, R. Azmi, T. Bergfeldt, S. S. Bhattacharya, R. Kruk, H. Hahn, S. Schweidler, T. Brezesinski, B. Breitung, *Sci. Rep.* **2020**, *10*, 18430.
- [40] C. Zhao, Q. Wang, Z. Yao, J. Wang, B. Sánchez-Lengeling, F. Ding, X. Qi, Y. Lu, X. Bai, B. Li, H. Li, A. Aspuru-Guzik, X. Huang, C. Delmas, M. Wagemaker, L. Chen, Y.-S. Hu, *Science* **2020**, *370*, 708.
- [41] a) J. Hafner, C. Wolverton, G. Ceder, *MRS Bull.* **2006**, *31*, 659; b) J. Hu, H. Shen, M. Jiang, H. Gong, H. Xiao, Z. Liu, G. Sun, X. Zu, *Nanomaterials* **2019**, *9*, 461.
- [42] a) M. I. Jordan, T. M. Mitchell, *Science* **2015**, *349*, 255; b) Y. Liu, O. C. Esan, Z. Pan, L. An, *Energy and AI* **2021**, *3*, 100049.
- [43] A. Chen, X. Zhang, Z. Zhou, *InfoMat* **2020**, *2*, 553.
- [44] a) P. K. Nayak, J. Grinblat, M. Levi, O. Haik, E. Levi, D. Aurbach, *J. Solid State Electrochem.* **2015**, *19*, 2781; b) A. Yu, G. V. Subba Rao, B. V. R. Chowdari, *Solid State Ionics* **2000**, *135*, 131; c) X. Jin, Q. Xu, H. Liu, X. Yuan, Y. Xia, *Electrochim. Acta* **2014**, *136*, 19; d) L. Croguennec, J. Bains, J. Bréger, C. Tessier, P. Biensan, S. Levasseur, C. Delmas, *J. Electrochem. Soc.* **2011**, *158*, A664; e) D. Wang, X. Li, Z. Wang, H. Guo, Y. Xu, Y. Fan, J. Ru, *Electrochim. Acta* **2016**, *188*, 48; f) Y. Gao, *Electrochem. Solid-State Lett.* **1999**, *1*, 117; g) K. C. Kam, A. Mehta, J. T. Heron, M. M. Doeff, *J. Electrochem. Soc.* **2012**, *159*, A1383; h) J. Kim, B. H. Kim, Y. H. Baik, P. K. Chang, H. S. Park, K. Amine, *J. Power Sources* **2006**, *158*, 641.
- [45] R. Pollice, G. dos Passos Gomes, M. Aldeghi, R. J. Hickman, M. Krenn, C. Lavigne, M. Lindner-D'Addario, A. Nigam, C. T. Ser, Z. Yao, A. Aspuru-Guzik, *Acc. Chem. Res.* **2021**, *54*, 849.
- [46] G. Ceder, Y. M. Chiang, D. R. Sadoway, M. K. Aydinol, Y. I. Jang, B. Huang, *Nature* **1998**, *392*, 694.
- [47] a) M. Guilmard, A. Rougier, M. Grüne, L. Croguennec, C. Delmas, *J. Power Sources* **2003**, *115*, 305; b) F. Dogan, J. T. Vaughey, H. Iddir, B. Key, *ACS Appl. Mater. Interfaces* **2016**, *8*, 16708.
- [48] L. Zou, J. Li, Z. Liu, G. Wang, A. Manthiram, C. Wang, *Nat. Commun.* **2019**, *10*, 3447.
- [49] C. Liang, F. Kong, R. C. Longo, C. Zhang, Y. Nie, Y. Zheng, K. Cho, *J. Mater. Chem. A* **2017**, *5*, 25303.
- [50] J. Lee, A. Urban, X. Li, D. Su, G. Hautier, G. Ceder, *Science* **2014**, *343*, 519.
- [51] Q. Zhang, J. Zhang, N. Li, W. Chen, *J. Appl. Phys.* **2019**, *126*, 025101.
- [52] B. Ye, T. Wen, M. C. Nguyen, L. Hao, C.-Z. Wang, Y. Chu, *Acta Mater.* **2019**, *170*, 15.
- [53] R. Feng, P. K. Liaw, M. C. Gao, M. Widom, *npj Comput. Mater.* **2017**, *3*, 50.
- [54] H. Xiang, Y. Xing, F.-z. Dai, H. Wang, L. Su, L. Miao, G. Zhang, Y. Wang, X. Qi, L. Yao, H. Wang, B. Zhao, J. Li, Y. Zhou, *J. Adv. Ceram.* **2021**, *10*, 385.
- [55] G. R. Schleder, A. C. M. Padilha, C. M. Acosta, M. Costa, A. Fazzio, *J. Phys.: Mater.* **2019**, *2*, 032001.
- [56] a) W. Huang, P. Martin, H. L. Zhuang, *Acta Mater.* **2019**, *169*, 225; b) Y. Zhang, C. Wen, C. Wang, S. Antonov, D. Xue, Y. Bai, Y. Su, *Acta Mater.* **2020**, *185*, 528; c) Z. Zhou, Y. Zhou, Q. He, Z. Ding, F. Li, Y. Yang, *npj Comput. Mater.* **2019**, *5*, 128; d) S. Y. Lee, S. Byeon, H. S. Kim, H. Jin, S. Lee, *Mater. Des.* **2021**, *197*, 109260.
- [57] Y. Yao, Z. Liu, P. Xie, Z. Huang, T. Li, D. Morris, Z. Finfrook, J. Zhou, M. Jiao, J. Gao, Y. Mao, J. Miao, P. Zhang, R. Shahbazian-Yassar, C. Wang, G. Wang, L. Hu, *Sci. Adv.* **2020**, *6*, eaaz0510.
- [58] a) Y. V. Krishna, U. K. Jaiswal, R. M. R., *Scripta Materialia* **2021**, *197*, 113804; b) D. Q. Zhao, S. P. Pan, Y. Zhang, P. K. Liaw, J. W. Qiao, *Appl. Phys. Lett.* **2021**, *118*, 231904.
- [59] a) N. Sarmadian, R. Saniz, B. Partoens, D. Lamoën, K. Volety, G. Huyberechts, J. Paul, *Phys. Chem. Chem. Phys.* **2014**, *16*, 17724; b) M. Aykol, S. Kim, V. I. Hegde, D. Snyder, Z. Lu, S. Hao, S. Kirklin, D. Morgan, C. Wolverton, *Nat. Commun.* **2016**, *7*, 13779.
- [60] G. Hautier, C. C. Fischer, A. Jain, T. Mueller, G. Ceder, *Chem. Mater.* **2010**, *22*, 3762.
- [61] J. G. Freeze, H. R. Kelly, V. S. Batista, *Chem. Rev.* **2019**, *119*, 6595.
- [62] a) J.-W. Yeh, *JOM* **2013**, *65*, 1759; b) B. Cantor, *Prog. Mater. Sci.* **2021**, *120*, 100754; c) J.-W. Yeh, S.-J. Lin, *J. Mater. Res.* **2018**, *33*, 3129.
- [63] a) F. Zhang, C. Zhang, S. L. Chen, J. Zhu, W. S. Cao, U. R. Kattner, *Calphad* **2014**, *45*, 1; b) B. Burger, P. M. Maffettone, V. V. Gusev, C. M. Aitchison, Y. Bai, X. Wang, X. Li, B. M. Alston, B. Li, R. Clowes, N. Rankin, B. Harris, R. S. Sprick, A. I. Cooper, *Nature* **2020**, *583*, 237; c) Y. Zhang, Y. J. Zhou, J. P. Lin, G. L. Chen, P. K. Liaw, *Adv. Eng. Mater.* **2008**, *10*, 534.
- [64] D. P. Tabor, L. M. Roch, S. K. Saikin, C. Kreisbeck, D. Sheberla, J. H. Montoya, S. Dwaraknath, M. Aykol, C. Ortiz, H. Tribukait,

- C. Amador-Bedolla, C. J. Brabec, B. Maruyama, K. A. Persson, A. Aspuru-Guzik, *Nat. Rev. Mater.* **2018**, 3, 5.
- [65] T. Gebhardt, D. Music, T. Takahashi, J. M. Schneider, *Thin Solid Films* **2012**, 520, 5491.
- [66] A. Ludwig, *npj Comput. Mater.* **2019**, 5, 70.
- [67] R. Potyrailo, K. Rajan, K. Stoewe, I. Takeuchi, B. Chisholm, H. Lam, *ACS Comb. Sci.* **2011**, 13, 579.
- [68] Z. Li, M. A. Najeeb, L. Alves, A. Z. Sherman, V. Shekar, P. Cruz Parrilla, I. M. Pendleton, W. Wang, P. W. Nega, M. Zeller, J. Schrier, A. J. Norquist, E. M. Chan, *Chem. Mater.* **2020**, 32, 5650.
- [69] L. Velasco, J. S. Castillo, M. V. Kante, J. J. Olaya, P. Friederich, H. Hahn, *Adv. Mater.* **2021**, 2102301, <https://doi.org/10.1002/adma.202102301>.
- [70] C. Wen, Y. Zhang, C. Wang, D. Xue, Y. Bai, S. Antonov, L. Dai, T. Lookman, Y. Su, *Acta Mater.* **2019**, 170, 109.
- [71] a) J. Kirman, A. Johnston, D. A. Kuntz, M. Askerka, Y. Gao, P. Todorović, D. Ma, G. G. Privé, E. H. Sargent, *Matter* **2020**, 2, 938; b) K. Higgins, S. M. Valletti, M. Ziatdinov, S. V. Kalinin, M. Ahmadi, *ACS Energy Lett.* **2020**, 5, 3426; c) S. Sun, A. Tihihonen, F. Oviedo, Z. Liu, J. Thapa, Y. Zhao, N. T. P. Hartono, A. Goyal, T. Heumueller, C. Batali, A. Encinas, J. J. Yoo, R. Li, Z. Ren, I. M. Peters, C. J. Brabec, M. G. Bawendi, V. Stevanovic, J. Fisher, T. Buonassisi, *Matter* **2021**, 4, 1305.
- [72] S. Langner, F. Häse, J. D. Perea, T. Stubhan, J. Hauch, L. M. Roch, T. Heumueller, A. Aspuru-Guzik, C. J. Brabec, *Adv. Mater.* **2020**, 32, 1907801.
- [73] H. S. Stein, J. M. Gregoire, *Chem. Sci.* **2019**, 10, 9640.
- [74] a) K. Kennedy, T. Stefansky, G. Davy, V. F. Zackay, E. R. Parker, *J. Appl. Phys.* **1965**, 36, 3808; b) J. J. Hanak, *J. Mater. Sci.* **1970**, 5, 964; c) Y. Han, B. Matthews, D. Roberts, K. R. Talley, S. R. Bauers, C. Perkins, Q. Zhang, A. Zakutayev, *ACS Comb. Sci.* **2018**, 20, 436; d) X. D. Xiang, X. Sun, G. Briceño, Y. Lou, K.-A. Wang, H. Chang, W. G. Wallace-Freedman, S.-W. Chen, P. G. Schultz, *Science* **1995**, 268, 1738; e) E. D. Specht, A. Rar, G. M. Pharr, E. P. George, P. Zschack, H. Hong, J. Ilavsky, *J. Mater. Res.* **2003**, 18, 2522.
- [75] A. Rar, J. J. Frafjord, J. D. Fowlkes, E. D. Specht, P. D. Rack, M. L. Santella, H. Bei, E. P. George, G. M. Pharr, *Meas. Sci. Technol.* **2004**, 16, 46.
- [76] a) Z.-W. Huang, K.-S. Chang, *Ceram. Int.* **2021**, 47, 22558; b) Y.-W. Chen, J.-J. Ruan, J.-M. Ting, Y.-H. Su, K.-S. Chang, *Ceram. Int.* **2021**, 47, 11451; c) A. Sarkar, R. Djenadic, N. J. Usharani, K. P. Sanghvi, V. S. K. Chakravadhanula, A. S. Gandhi, H. Hahn, S. S. Bhattacharya, *J. Eur. Ceram. Soc.* **2017**, 37, 747; d) M. Biesuz, L. Spiridigliozzi, G. Dell'Agli, M. Bortolotti, V. M. Sglavo, *J. Mater. Sci.* **2018**, 53, 8074.
- [77] a) C. Neuber, M. Bäte, M. Thelakkt, H.-W. Schmidt, H. Hänsel, H. Zettl, G. Krausch, *Rev. Sci. Instrum.* **2007**, 78, 072216; b) J. C. Grunlan, A. R. Mehrabi, A. T. Chavira, A. B. Nugent, D. L. Saunders, *J. Comb. Chem.* **2003**, 5, 362; c) A. Saeki, K. Kranthiraja, *Jpn. J. Appl. Phys.* **2019**, 59, SD0801; d) R. Gómez-Bombarelli, J. Aguilera-Iparraguirre, T. D. Hirzel, D. Duvenaud, D. Maclaurin, M. A. Blood-Forsythe, H. S. Chae, M. Einzinger, D.-G. Ha, T. Wu, G. Markopoulos, S. Jeon, H. Kang, H. Miyazaki, M. Numata, S. Kim, W. Huang, S. I. Hong, M. Baldo, R. P. Adams, A. Aspuru-Guzik, *Nat. Mater.* **2016**, 15, 1120; e) M. Saliba, *Adv. Energy Mater.* **2019**, 9, 1803754; f) G. Kumar, H. Bossert, D. McDonald, A. Chatzidimitriou, M. A. Ardagh, Y. Pang, C. Lee, M. Tsapatsis, O. A. Abdelrahman, P. J. Dauenhauer, *Matter* **2020**, 3, 805.
- [78] E. M. Chan, C. Xu, A. W. Mao, G. Han, J. S. Owen, B. E. Cohen, D. J. Milliron, *Nano Lett.* **2010**, 10, 1874.
- [79] B. P. MacLeod, F. G. L. Parlange, T. D. Morrissey, F. Häse, L. M. Roch, K. E. Dettelbach, R. Moreira, L. P. E. Yunker, M. B. Rooney, J. R. Deeth, V. Lai, G. J. Ng, H. Situ, R. H. Zhang, M. S. Elliott, T. H. Haley, D. J. Dvorak, A. Aspuru-Guzik, J. E. Hein, C. P. Berlinguette, *Sci. Adv.* **2020**, 6, eaaz8867.
- [80] Y. Hu, B. Liu, Y. Wu, M. Li, X. Liu, J. Ding, X. Han, Y. Deng, W. Hu, C. Zhong, *Front. Chem.* **2020**, 8, 579828.
- [81] M. Matsubara, A. Suzumura, N. Ohba, R. Asahi, *Commun. Mater.* **2020**, 1, 5.
- [82] S. Shuang, H. Li, G. He, Y. Li, J. Li, X. Meng, *Rev. Sci. Instrum.* **2019**, 90, 083904.
- [83] G. Song, Z. Liu, F. Zhang, F. Liu, Y. Gu, Z. Liu, Y. Li, *J. Mater. Chem. C* **2020**, 8, 3655.
- [84] T. A. Stegk, R. Janssen, G. A. Schneider, *J. Comb. Chem.* **2008**, 10, 274.
- [85] a) Z. Li, A. Ludwig, A. Savan, H. Springer, D. Raabe, *J. Mater. Res.* **2018**, 33, 3156; b) A. Ludwig, R. Zarnetta, S. Hamann, A. Savan, S. Thienhaus, *Int. J. Mater. Res.* **2008**, 99, 1144; c) J. C. Zhao, X. Zheng, D. G. Cahill, *Mater. Today* **2005**, 8, 28.
- [86] S. Kumari, J. R. C. Junqueira, W. Schuhmann, A. Ludwig, *ACS Comb. Sci.* **2020**, 22, 844.
- [87] N. M. Al Hasan, H. Hou, S. Sarkar, S. Thienhaus, A. Mehta, A. Ludwig, I. Takeuchi, *Engineering* **2020**, 6, 637.
- [88] a) Y. Xu, Y. Bu, J. Liu, H. Wang, *Scr. Mater.* **2019**, 160, 44; b) S. Guerin, B. E. Hayden, *J. Comb. Chem.* **2006**, 8, 66.
- [89] A. Sarkar, R. Djenadic, D. Wang, C. Hein, R. Kautenburger, O. Clemens, H. Hahn, *J. Eur. Ceram. Soc.* **2018**, 38, 2318.
- [90] a) A. Sarkar, B. Eggert, L. Velasco, X. Mu, J. Lill, K. Ollefs, S. S. Bhattacharya, H. Wende, R. Kruk, R. A. Brand, H. Hahn, *APL Mater.* **2020**, 8, 051111; b) M. R. Chellali, A. Sarkar, S. H. Nandam, S. S. Bhattacharya, B. Breitung, H. Hahn, L. Velasco, *Scr. Mater.* **2019**, 166, 58.
- [91] J. K. Pedersen, T. A. A. Batchelor, A. Bagger, J. Rossmeisl, *ACS Catal.* **2020**, 10, 2169.
- [92] T. Hasegawa, T. Kageyama, T. Fukumura, N. Okazaki, M. Kawasaki, H. Koinuma, Y. K. Yoo, F. Duerwer, X.-D. Xiang, *Appl. Surf. Sci.* **2002**, 189, 210.



Qingsong Wang is a postdoctoral researcher at INM—Leibniz Institute for New Materials in Saarbrücken, Germany. He is currently a guest scientist at Institute of Nanotechnology (INT), Karlsruhe Institute of Technology (KIT), Germany. He received his Ph.D. degree in Materials Physics and Chemistry from Shanghai Institute of Ceramics, Chinese Academy of Sciences in 2016. His research interests focus on solid state electrolytes and high entropy materials for energy storage and conversion.



Leonardo Velasco is a group leader at the Institute of Nanotechnology (INT), Karlsruhe Institute of Technology. He obtained his Ph.D. in Materials Science from the University of Southern California in 2016. Later on, he joined the nanostructured materials unit at the INT, working on synthesis and characterization of high entropy materials. Since 2019, he introduced the automation of equipment for the development of high throughput synthesis and characterization of multicomponent materials. Additionally, he works on mechanical and transport properties of dense materials produced by physical vapor deposition techniques.



Ben Breitung is group leader at the Institute of Nanotechnology, Karlsruhe Institute of Technology. He obtained his Ph.D. in 2013, and then joined the Battery and Electrochemistry Laboratory (BELLA). Since 2018, he is working on his habilitation project and explores high-entropy materials for various electrochemical applications. Besides electrode materials, other functional materials for catalytic, sensor, and electronic applications are subjects of his work.



Volker Presser is full professor at Saarland University and Program Division Leader at the INM—Leibniz Institute for New Materials (both in Saarbrücken, Germany). He received his doctorate with distinction in Applied Mineralogy from the Eberhard-Karls University (Tübingen, Germany) in 2009. His work explores electrochemical materials and processes for energy storage, water remediation, energy harvesting, and ion separation.